1 **Carbon nanoparticle exposure strengthens water-relation parameters by stimulating**
2 **abscisic acid pathway and aquaporins genes in rice**

3 Aman Kumar[1], Lekshmi Manasa S[13], Jyotiprabha Kashyap[1], Sikha Mandal[4], Gayatri Mishra[6] Jnanendra Rath[5],
4 Gyana Ranjan Rout[7], Kishore CS Panigrahi[1‡], Madhusmita Panigrahy[127*]

5 [1]National Institute of Science Education and Research (NISER), Homi Bhabha National Institute (HBNI),
6 752050, Khurda, Jatni, India

7 [2]Biofuel & Bioprocessing Research Centre, ITER, Siksha 'O' Anusandhan University, India, 751002

8 [3]Department of Agricultural Biotechnology, Odisha University of Agriculture & Technology, Bhubaneswar
9 751003, Odisha, India

10 [4]Dept. of Botany, Sree Chaitanya College, Habra, sikhasm@gmail.com

11 [5]Department of Botany, Institute of Science, Visva-Bharati (A Central University), Santiniketan, West Bengal –
12 731235

13 [6]U. S. Department of Agriculture (USDA) Forest Service, University of Utah, United States of America

14 [7]Department of Molecular Biology & Biotechnology, Institute of Agricultural Sciences, Siksha 'O' Anusandhan
15 University, 751029, India

16 *Corresponding Author

17 Madhusmita Panigrahy, E Mail: mpanigrahy@niser.ac.in, madhusmitapanigrahy@soa.ac.in, Phone: +91-
18 8762086581, Orcid ID: 0000-0001-8153-014X

19 ‡Co-Corresponding Author

20 Kishore CS Panigrahi, E Mail: panigrahi@niser.ac.in, Phone: +91-0674-2494140, Orchid ID: 0000-0002-1855-
21 7777

22 **ABSTRACT**

23 Mechanism of action and molecular basis of positive growth effects including yield increase due to
24 carbon nanoparticle (CNP) treatment in rice plants is dissected here. CNP at 500 -750 µg/mL were found to be
25 the optimum dosages showing best seedling growth. CNP treatment resulted increase in stomata size, gaseous
26 exchange and water use efficiency along with decrease in stomata frequency, relative humidity, internal CO_2
27 concentration. CNP treatment exerted cold tolerance in seedlings and water stress tolerance in reproductive stage.
28 CNP-coupled with water uptake was found to be endocytosis mediated, although CNP uptake was not affected by
29 endocytosis inhibitor application in roots. Genomic analysis resulted major involvement of ABA pathway and
30 stomata size and frequency genes in *Arabidopsis* and rice. Elevated endogenous ABA in rice seedlings and flag
31 leaves along with increased expression of ABA biosynthetic genes in *Arabidopsis* and rice *AtNCED3*, *AtNCED6*,
32 *OsNCED1* confirmed increased ABA synthesis. Negative regulators of ABA pathway, *OsSNRK2* down-regulation
33 and up-regulation of stomagen (*OsEPFL9*) reconfirmed ABA's involvement. CNP treatment resulted water stress
34 tolerance by maintaining lower stomatal conductance, transpiration rate and higher relative water content.
35 Increased ABA (*OsSNRK1*, *OsSNRK2*) and aquaporin (*OsPIP2-5*) genes' expressions could explain the better
36 water stress tolerance in rice plants treated with CNP. Altogether, due to thermomorphogenesis, down-regulation
37 of Phytochrome B resulted altered the ABA pathway and stomatal distribution with size. These changes resulted
38 improved water relation parameters and WUE showing improvement in yield. Detailed mechanism of action of
39 CNP in abiotic stress tolerance can be exploited in in nano-agriculture.

40 **Key Words:** Carbon Nanoparticle, Rice, Arabidopsis, Drought, Water stress, Abscisic acid, Stomata

41 **Introduction**

42 Use of nanomaterials for improvement in agriculture is known as nano agriculture and the technologies exploited
43 for these purposes are together called nanotechnology. Nano agriculture in this emerging era has proved as a
44 potential tool to solve several problems faced in agriculture (Mazeed et al., 2020). The multifaceted solutions

45   offered by nano agriculture include avoiding excessive use of pesticides in crops, increased growth and yield of
46   crops, targeted delivery of DNA at the site of application, improved nutrient use efficiency, detection of diseases
47   by the use of nanosensors etc. (Rani et al., 2020). Use of nano materials greatly effects the plant species through
48   different pathways and influences their effectiveness. Hence, the method of their application is very critical to
49   meet the expectations (Alejandro, 2017). Equally important is to understand how the nanomaterials are absorbed,
50   transported, internalized and brings its effect in the plant species in which they are applied. As it strengthens the
51   fundamentals of the mechanisms involved and clarifies the issues related to wide acceptance of the method. Recent
52   reports have also started to explore the mechanisms underlaying and the working principles of the nano materials
53   inside plants of use. Studies have attempted to address the molecular mechanisms of nano toxicity using
54   differential protein expression profiling, genomics approaches, microRNA analysis and nanotoxicoproteomics
55   approaches (Jha et al. 2016). Studies have shown that in addition to the internal use of nanomaterials, their external
56   application in the growth medium can also induce growth effects without toxicity issues. External application
57   methods of engineered or non-engineered nanomaterials include foliar spray, hydroponics, seed priming, and in
58   soil (Zhao et al., 2020). External application of multi walled carbon nanotubes (MWCNT) in the growth medium
59   enhanced seed germination and growth by exhilarating expression of several aquaporins, plasma membrane
60   intrinsic proteins and tonoplast intrinsic proteins (Lahiani et al., 2013). In our previous report, genetic mechanisms
61   associated with external application carbon nanoparticle (CNP) in the growth medium of *Arabidopsis* resulted
62   accelerated flowering, photoperiod dependence and shade avoidance (SAR)-like effects with down-regulation of
63   red-light photoreceptor Phytochrome B's transcript levels (Kumar et al., 2018). This was probably the first report
64   elucidating links of the mechanisms of CNP with another physiological syndrome such as SAR and light
65   signalling. Nanoparticle exposure have also been greatly exploited to attain robust growth and yield in different
66   plant species (Zhao et al., 2020). Our effort to test the effect of CNP external application in the rice pots resulted
67   improvement in growth and yield of rice plants (Panigrahy et al., 2021). The analyses of underlaying mechanisms
68   revealed hike of plant internal temperature by $0.5°C \pm 0.1°C$ due to the presence of CNP which could mimic the
69   situation of shade and stimulated SAR in rice plants. Several recent studies have also successfully attempted to
70   attain abiotic and biotic stress tolerance through external application of nanomaterials in plants (Ali et al. 2021,
71   Majeed et al., 2020). An et al. have shown salinity tolerance in cotton by application of cerium oxide nanoparticles
72   in the germinating medium (An et al., 2020). Hatami et al. showed improved drought tolerance in *Hyoscyamus*
73   seedlings due to 14-days exposure to SWCNT under different levels drought induced by polyethylene glycol
74   (Hitami et al., 2017). Despite so many analyses and advantages obtained from nanomaterials application, detailed
75   study including natural environmental conditions covering full life cycle of a plant and addressing the nutritional
76   quality of the grains obtained are scanty. Effect of cerium oxide nanoparticles on the rice grain quality was shown
77   by Rico et al., (2013). Beneficial effects of copper oxide nanoparticles in rice at filed level with their effect on
78   grain was shown by Deng et al., (2022). Our previous results demonstrated that CNP exposure in rice pots
79   improved the nutritional quality of the rice grains obtained from the CNP-treated plants. In the present study we
80   have investigated the molecular basis of action of CNP to exert the growth effects in rice. We have also accessed
81   different abiotic stresses to find which abiotic stress tolerance CNP can induce in rice plants. Further, molecular,
82   genetic as well as genomic analyses have been attempted to answer the basis of drought tolerance in rice plants
83   that we obtained due to CNP exposure.

Result

Dosage dependence effect of CNP on the rice seedlings' phenotypic growth

86   CNP had induced several positive growth effects in rice plants (Panigrahy et al., 2021). Hence, it was necessary
87   to determine the ineffective, optimum and maximum concentrations of CNP to show positive growth effects.
88   Study of seedling shoot length (SL), root length (RL), rootlet number (RLN) and nodal roots (NR) at 7 different
89   CNP concentrations (ranging from 200 µg/ml to 1500 µg/ml) (Figure 1, Suppl Figure 1) showed that SL, RL and
90   RLN tend to increase after at least 350 µg/ml indicating positive growth effects. SL and RL showed highest

91 increase between 500 and 750 µg/ml after which they started to decline (Figure 1A). RLN also was highest number
92 at 750 µg/ml (Figure 1).
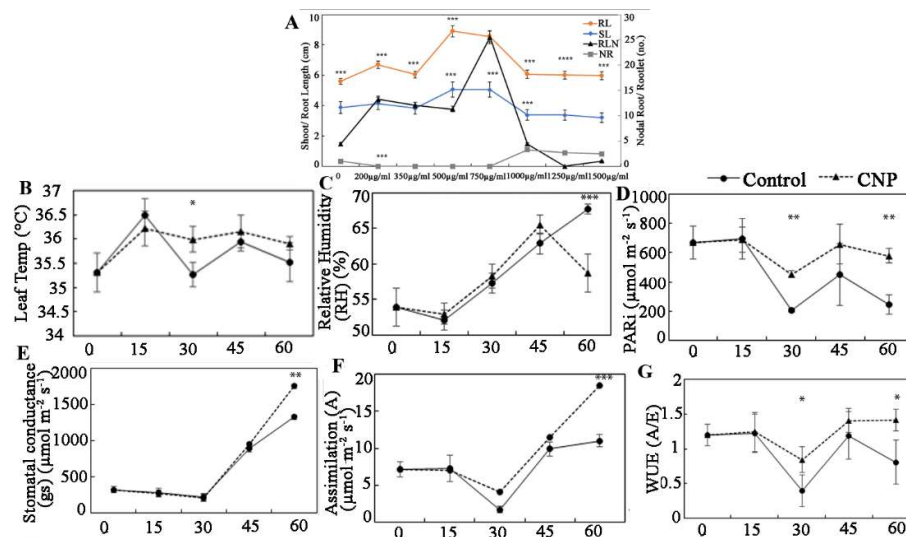
Figure 1. Dosage dependence effect and Leaf gaseous exchange, water relation parameters of CNP exposure

(A): Dosage dependence effect of Carbon nanoparticle exposure on seedling growth. Seedlings were grown on 50 ml Murashige and Skoog (MS) medium containing different concentration of CNP including 200, 350, 500, 750, 1000, 1250 and 1500 µg/mL) for 7 d. On the 8th day, seedling growth parameters such as shoot length (SL), root length (RL), rootlet number (RLN), Nodal roots (NR) were measured. All data presented were from minimum 30 seedlings in each experiment with 2 replications. Significances of values were obtained from one-way ANOVA using the Turkey's multiple comparison in the Prism version 7.0 software, and were represented as ***, $P \leq 0.001$. (B-G): Leaf gaseous exchange and water relation parameters in the CNP-treated rice plants. Leaf gaseous exchange, water relation and photosynthetic parameters were recorded in CNP-treated and untreated plants before each of the four CNP treatments on the 45th, 60th, 75th, 90th after sowing (DAS). The last reading was taken 15 days after the last treatment on 90th day (on the 125th day). Thus, the 45th, 60th, 75th, 90th, 125th day measurements were noted as 0-day, 15th-day, 30th -day, 45th -day and 60th -day of CNP-treatment respectively. The middle part of top second leaf was used for taking readings. Each data point in the graph is a mean of 108 recordings with 6 plants from each either untreated or CNP-treated plants. For each plant 18 recordings were done from 3 leaves in time series of 5 seconds interval, with 6 readings from each leaf. PAR: Photosynthetically actinic radiation, A: Assimilation, GS: stomatal conductance, E: transpiration rate, VPD: vapour pressure deficit, Ci: CO_2 concentration inside the leaf, WUE: water use efficiency. Significances of values were obtained from one-way ANOVA using the Turkey's multiple comparison in the Prism version 7.0 software, and were represented as *, $P \leq 0.05$, **, $P \leq 0.01$ and ***, $P \leq 0.001$.

These results indicated that the optimum concentration of CNP on rice seedlings were between 500 and 750 µg/ml. NR showed opposite trend with in increase after at least 750 µg/ml and was higher till 1500 µg/ml of CNP (Figure 1). This further indicated that NR could be a toxicity response induced due to CNP between 1000 - 1500 µg/ml. Germination percentage on 4th day of rice seeds was homogenously 100% in all concentration indicating that CNP didn't exert any effect on seed germination or growth of seedlings.

Effect of CNP treatment on physiological parameters in rice plants

Water relation parameters were assessed after four CNP treatments in the treated and untreated plants to investigate the reason of improved growth and yield of CNP-treated plants (Figure 1B-G)). Photosynthesis parameters such as photosynthetically active radiation inside the leaf (PARi) (Figure 1D), carbon assimilation (A) (Figure 1F) showed significantly higher values in the CNP-treated plants. Water relation parameters such as leaf

124 temperature (Tleaf) (Figure 1B), and water use efficiency (WUE) (Figure 1G) were significantly higher (by 0.4°C
125 ± 0.1°C and 75% respectively) in the CNP-treated plants. Relative humidity (RH) (Figure 1C) was significantly
126 less (i.e. 13.3%) in CNP-treated plants. Vapour pressure deficit (VPD) (Figure 2F) and transpiration rate (E)
127 showed negligible changes between the CNP-treated and the control plants (data not shown). Stomatal
128 conductance was also found to be higher in the CNP-treated plants (Figure 1E). CIRASS3 measurements and
129 analysis showed improvements in the water relation traits in the CNP treated plants as compared to their controls.

130 **Effect of CNP treatment on stomatal parameters in rice plants**

131 As the CNP-treated plants had improved water relation parameters, stomatal analysis was performed using
132 confocal microscopy in the control and CNP-treated samples in the seedlings stage as well as after 4th CNP
133 treatment in plants (Figure 2).

134
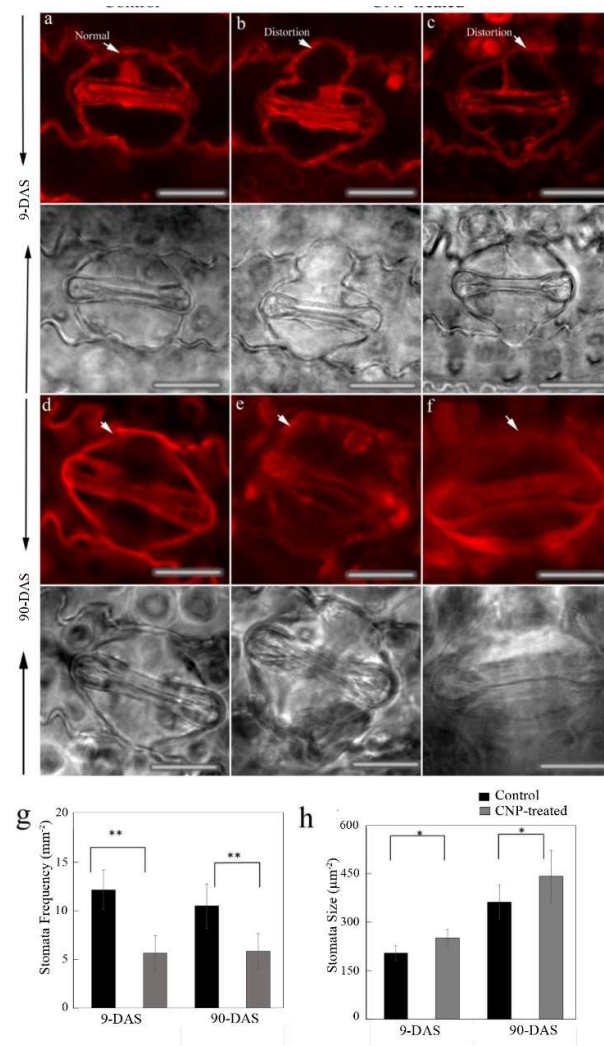
135 **Figure 2. Confocal Microscopic analysis of stomata and cell wall in the CNP-treated rice plants.** Leaf Tissue
136 samples from 9d-old seedlings (9 DAS) or 90d-old plants (after 4th CNP treatment) (90 DAS) were fixed with
137 FAA substituted with methanol and stained with propidim iodide to visualize cell wall of stomatal guard cells.
138 Middle portion of the top second leaf was used in case of adult samples. Arrow marks indicate distortions in CNP-
139 treated plants. (A-C): seedlings, (D-F): adult plant leaf. Each representative plant image is placed with its
140 corresponding bright field image below. Scale Bar: 10 µM. G: stomata frequency and H: stomatal size. Size and
141 frequency of stomata were averaged from 6 leaf sections in either control or CNP treated with n≥30.

4

142

143   Stomata in the seedling cells showed clear bulging in the cell wall and distortions of the CNP-treated samples
144   which were completely absent in the control samples (Figure 2A-2C). Samples from older plants also showed
145   similar bulging and distortions (Figure 2D-2F). Frequency of stomata per unit area of leaf decreased significantly
146   (~50%) in both the seedlings and older plant leaves (Figure 2G) with an increase of ~6% in the size of the stomata
147   (Figure 2H). These results indicated that CNP treatment might have affected to increase stomatal size and decrease
148   in their frequency.

149   **Analysis of mechanism of CNP uptake**

150   Water uptake by the seedlings with or without CNP in the medium was quantified studying the % increase or
151   decrease of water uptake per seedling (Figure 3).
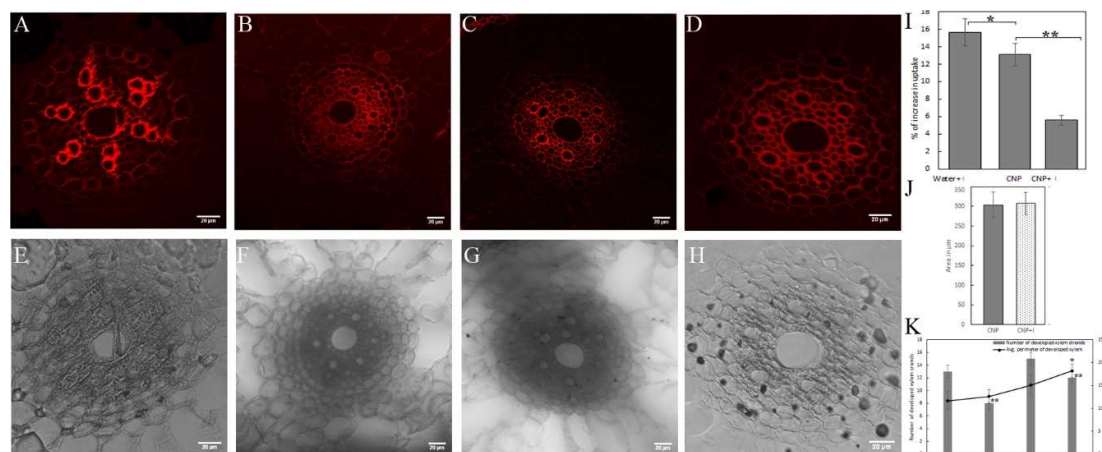

152

153   **Figure 3. Analysis of CNP-water uptake mechanism in to plant roots.** Root tissue samples from 9d-old
154   seedlings with or without CNP treatment were grown in water in air tight plantons. Water uptake/ seedling was
155   calculated as described in materials and methods from water left in the planton and seedling weight. For xylem
156   perimeter and number root samples were fixed, moulded, embedded and sectioned prior to confocal microscopy.
157   CNP aggregates and xylem were analysed from confocal images using Image J software. Data represents mean
158   of 15 focuses at microscope generates from 3 biological replicate root samples in each case. Significances of
159   values were obtained from one-way ANOVA using the Turkey's multiple comparison in the Prism version 7.0
160   software, and are represented as *, $P \leq 0.05$, **, $P \leq 0.01$.

161

162   Addition of CNP in the medium increased water uptake (i.e., 13%) by the seedlings (Figure 3I). To understand if
163   CNP uptake is coupled to water uptake or through exo-/ endo- or pinocytosis, inhibitor nocodazole was added
164   with or without CNP in the medium. Treatment with nocodazole increased the water uptake by 16% than the
165   control with water alone (Figure 3I). Nocodazole treatment in the CNP-treated seedlings reduced the water uptake
166   (6% more than control water alone) as compared to those CNP treated ones (Figure 3I). To investigate the reason
167   of increased water uptake with CNP, number of developed xylem strands and their average perimeter was
168   measured from confocal microscopy images in CNP-treated root samples. Control seedlings with water alone
169   showed 13±1 developed xylem strands with an average perimeter of ~11.6 μm (Figure 3A, 3E, 3K). Seedlings
170   grown with nocodazole showed reduced number (i.e., 8±1) of developed xylem strands but no change in average
171   perimeter (Figure 3B, 3F, 3K). CNP-treated seedlings showed increase in number of developed xylems (i.e., 14-
172   15 ±1), which were found in 2-3 rings also with increased average perimeter of developed xylem strands of ~15
173   μm (Figure 3C, 3G, 3K). Inhibitor application with CNP treatment showed similar number of developed xylem
174   strands as that of CNP, however the average diameter was reduced to ~10.9 μm indicating reduced water uptake
175   ((Figure 3D, 3H, 3K). Further, an estimate of CNP uptake was made by measuring the area of CNP aggregates in
176   the confocal microscopy images. CNP aggregates in the nocodazole treated samples similar to that with the CNP-
177   treatment alone (Figure 3J).

Genome-wide expression and pathway analysis of transcripts during CNP-treatment

Our first report in *Arabidopsis thaliana* (*A.thaliana*; At) plants with CNP treatment induced accelerated flowering, photoperiod dependency (Kumar et al., 2018) and in our second study on rice, CNP treatment resulted improved growth and yield along with shade avoidance response (SAR) phenotype and increased plant temperature, albeit with minimal preponement of flowering time (Panigrahy et al., 2021). To understand the basis of the differences in CNP effects in the model dicot and monocot plants, transcriptome analysis and microarray experiment was performed separately from seedling or leaf samples of *A. thaliana* and flag leaf samples of Swarna rice variety respectively (Figure 4).
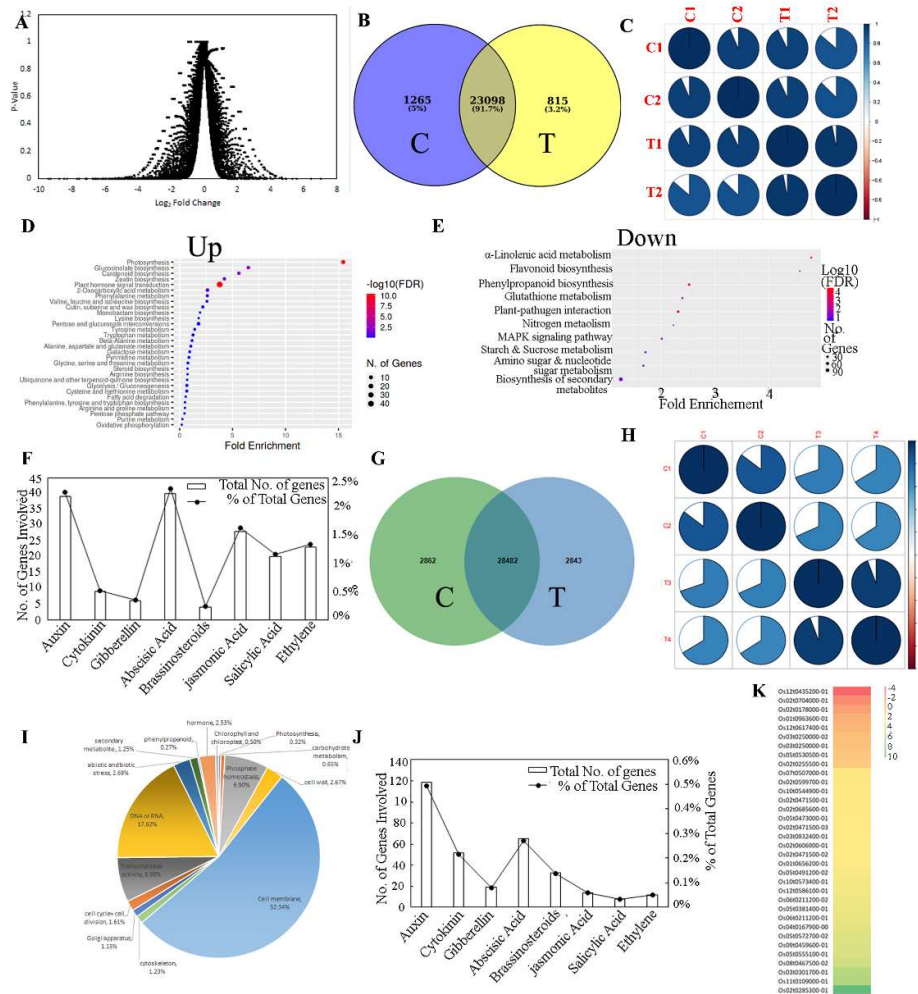
Figure 4. Genome-wide expression analysis in CNP-treated seedlings in rice and *Arabidopsis*. (A-D): Transcriptome sequencing analysis data from *Arabidopsis.* Seedlings were grown on medium without or with 500 μg/ml CNP and sampled on 16th day. (E-H): Microarray gene expression analysis data from rice flag leaf samples on the day of full panicle emergence after 4th CNP treatment. (A): volcano plot of DEG with $\log_2$ FC cut off 1.0 and P≤0.05, (B): Venn diagram of number of DEG identified, (C-D): Dot plots showing fold enrichment of up and down-DEG, (E): Pathway analysis of eight plant growth hormones in the transcriptome sequencing data (F): Correlation plot among replicates of control and CNP-treatment samples, (G): venn diagram of number of probes identified in microarray experiment, (H): Heat map of 34 selected ABA pathway genes from the microarray data. (I): Pathway analysis of eight plant growth hormones in the microarray DEGs

197 Each of these experiments were done with 2 biological replicates from control condition or with CNP. At
198 transcriptome volcano plot for transcripts below 1.0 (Figure 4A) showed that highest number of transcripts
199 (37.4%) had p<0.5. Moreover, the replicates of control libraries or the test libraries bear more collinearity (Figure
200 4C), making them suitable platform for further analysis. Standard analysis of the transcripts (described in Methods
201 section) resulted 23098 differentially expressed transcripts (DEG) which were found in both with and without
202 CNP (Figure. 4B). Pathway enrichment analysis showed the fold-enrichment of the Up- or Down-regulated DEGs
203 (Figure 4D, 4E) with the number of genes of the top 30 pathways. Among the up-regulated DEGs, 'Plant hormone
204 signal transduction pathways' was highly enriched with fold enrichment 3.78, enrichment FDR value 3.77413E-
205 11 containing 40 genes in list (Figure 4D). And among the down-DEGs, unsaturated fatty acids such as 'α-
206 linolenic acid metabolism' (fold enrichment 4.79, enrichment FDR 1.68024E-05) followed by 'phenylpropanoid
207 biosynthesis' with fold enrichment of 2.52 and enrichment FDR of 5.02073E-05 were prominent (Figure 4E).
208 These results indicated that CNP treatment in *A.thaliana* alleviated lipids and secondary metabolites with
209 decreased alpha-linolenic acid like stress antioxidants. Moreover, it indicated an increased involvement of
210 hormone signal transduction. Pathway category analysis of At transcriptome DEGs showed that abscisic acid
211 (ABA) pathway genes were involved to the highest followed by the auxin pathway genes (Figure. 4F). Microarray
212 analysis from CNP-treated and untreated samples of Swarna rice flag leaf samples resulted 52% to 59% of
213 detection of probes in the control and test arrays, with 28,482 probes detected in common (Figure 4G). Collinearity
214 among the control and test replicates above 0.8 (Figure 4H) created suitable platform for further analysis.
215 Function and pathway analysis showed that major category of transcripts in the CNP-treated samples were from
216 cell membrane, DNA or RNA, transcriptional activity, phosphate homeostasis genes. Hormone pathway genes
217 acquired 2.53% of the total genes involved (Figure 4I). Cohering to the pathway result of *A.thaliana*, pathway
218 analysis of rice samples revealed that ABA pathway genes were highly enriched being the second most enriched
219 after auxin pathway genes (Figure. 4J). Out of the 34 most prominent ABA pathway genes, 29 were found to be
220 up-regulated in CNP-treated samples (Figure. 4K).

Comparative study of functional categories of differentially expressed genes (DEGs) among rice and *Arabidopsis*

223 DEGs from the *At* transcriptome and rice (*Os*) microarray were arranged according to their function (GO
224 annotation), pathway involved (KEGG database) and details obtained from TAIR and RAP-annotations for
225 *Arabidopsis* and rice respectively. These relevant categories included ABA pathway, cold stress response, light
226 signaling and circadian clock, photosynthesis and carbohydrate, ROS detoxification, ion and water transport,
227 stomata size, which were used for the comparative analysis among the two model plant systems (Table S1, Table
228 S2). In ABA pathway, 34 genes were found among which majority (24 genes) were up-regulated in rice. Whereas,
229 in *Arabidopsis* only 12 gene were found to be involved in ABA pathway, most of which (~66%) are down-
230 regulated. Cold stress response category of genes represented different regulation among *At* and *Os*. In rice ~54%
231 of these genes were up-regulated, whereas in *At* most of the genes in this category were down-regulated. Genes
232 of light signaling, and circadian clock didn't represent any significant differences in their numbers of up and down
233 DEGs among rice and *At*. In photosynthesis, chlorophyll and carbohydrate category, all the DEGs were down-
234 regulated in rice while ~63% of DEGs were up-regulated in *At*. DEGs of ROS detoxification category presented
235 contrasting pattern with majority being down-regulated in *At* and up-regulated in rice. However, the transcript
236 levels of superoxide dismutase and catalase in *At* data were upregulated (Table S2). Also, the 11 class III
237 Peroxidases found in rice microarray data were all up-regulated indicating these may act to detoxify the ROS in
238 CNP-treated samples. The DEGs of ion, solute and water transport category were synergistically presented being
239 majority of them down-regulated in both *At* and rice. DEGs of stomata size were up-regulated in both At and rice.
240 These results indicated that CNP treatment induced differential effect on regulation of genes of different functional
241 categories in *At* or rice.

Effect of CNP treatment on endogenous Abscisic acid content and synthesis

243 To understand if CNP treatment with abscisic acid (ABA) has any effect on seedling root and shoot growth,
244 (ABA) was added to the growth medium to observe its effect on seedling phenotype. ABA is known to slow down

7

245 the root and shoot growth in rice (Chen et al., 2006). ABA treatment without or with CNP resulted comparable %
246 of decrease in SL and RL respectively (Figure 5A).

247
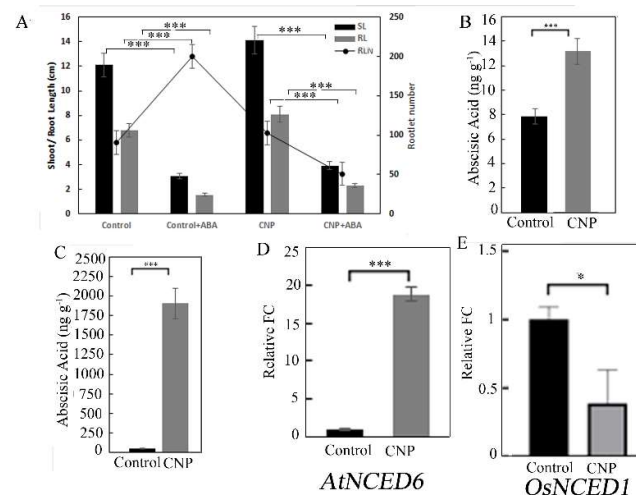
Figure 5. Effect of ABA treatment and endogenous ABA quantification in CNP-treated seedlings. (A)
248 Seedling phenotype was assayed in 14d-old seedlings after 10 μM ABA treatment on the 5th day. (B) Endogenous
250 ABA content was assayed in seedlings and (C) adult leaf samples. Top second leaf was used for lyophilization.
251 (B-C): data represented is a mean of three replicative measurements. Transcript expression levels of ABA
252 biosynthesis gene in (D) Arabidopsis *9-cis-epoxycarotenoid dioxygenase 5* (*AtNCED6*) and (E) rice *9-cis-*
253 *epoxycarotenoid dioxygenase 1* (*OsNCED1*) were determined using qRT-PCR. Transcript levels of ACTIN was
254 used to normalise transcript levels. Reactions were done in triplicates from two biological replicates. Data
255 represents as the mean ±SEM. The relative quantification of genes was analyzed using standard $2^{-\Delta\Delta ct}$ method. For
256 relative fold-change, the respective expression value for the same gene from untreated plant leaf samples was
257 taken as 1. Statistical significance was obtained from one-way ANOVA using the Turkey's multiple comparison
258 in the Prism version 7.0 software, and were represented as *, $P \leq 0.05$, **, $P \leq 0.01$ and ***, $P \leq 0.001$.

259

260 While SL decreased 74.6% and 72.2%, RL decreased 77.2% and 71.6% in case of control and CNP-treated
261 seedlings respectively (Figure 5A). RLN in the CNP-treated seedlings decreased to nearly half, however
262 surprisingly, the control seedlings showed significant increase of ~2.2-fold in the RLN with ABA treatment
263 (Figure 5A). These results indicated that CNP induced growth effects could alter endogenous ABA levels.
264 Endogenous ABA in seedlings showed that CNP-treated seedlings had nearly double amount of endogenous ABA
265 than the untreated ones (Figure 5B). Congruently, flag leaf samples of CNP-treated plants were found to have
266 ~40-fold higher ABA content than the untreated ones (Figure 5C). Additionally, the three other defense hormones
267 such as jasmonic acid (JA), salicylic acid (SA) and oxylipins (oxy) were also found to be higher in the CNP-
268 treated plants (Suppl. Figure 2). Transcript expression analysis of ABA biosynthesis gene *9-cis-epoxycarotenoid*
269 *dioxygenase 5* (*AtNCED6*) in *Arabidopsis* seedlings (Figure 5D) and *9-cis-epoxycarotenoid dioxygenase 1*
270 (*OsNCED1*) in rice flag leaves (Figure 5E) were validated to support the above observation of ABA content.
271 *AtNCED6* relative expression level was increased to ~18-fold and *OsNCED1* relative expression level was
272 decreased to ~0.39-fold after CNP treatment.

273 **Transcript expression analysis to understand CNP-treated plants' phenotype**

274 To have insights into CNP-treated plant's phenotype, transcript expression of different selected genes from
275 photosynthesis, calvin cycle, cold tolerance, stomata size and frequency, genes for ABA pathway were studied
276 using qPCR in CNP-treated plants in comparison with their control plants. The concordance of the transcript
277 expression levels of majority of the genes analysed from the rice microarray with the qRT-PCR fold change
278 provided evidence of sound genomic data set (Suppl. Figure 3A). Photosynthesis related gene *OXYGEN*

8

279   *EVOLVING COMPLEX1* (*OsOEE1*) was significantly down-regulated to 0.25-fold in CNP-treated samples
280   compared to the controls (Figure 6A).

281
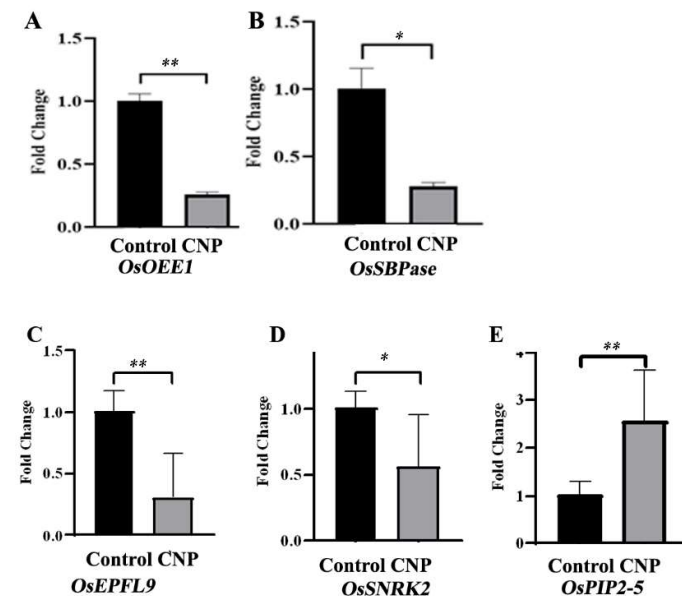
Figure 6. Transcript expression analysis in CNP-treated rice plant samples. Transcript expression levels of
genes involved in photosynthesis, cold tolerance, stomata and water relations were studied using qRT-PCR in flag
leaf samples after 4th CNP treatment. (A): *OXYGEN EVOLVING COMPLEX1* (*OsOEE1*), (B):
SEDOHEPTULOSE 1-7-BI-PHOSPHATE (OsSBPase), (C): *EPIDERMAL PATTERNING FACTOR-LIKE 9*
(*OsEPFL9*), (D): *SUCROSE NON-FERMENTING-1 RELATED PROTEIN KINASE 2* (*OsSNRK2*), (E) *PLASMA
MEMBRANE INTRINSIC PROTEIN 2-5* (*OsPIP2-5*). Transcript levels of ACTIN was used to normalise transcript
levels. Reactions were done in triplicates from two biological replicates. Data represents as the mean ±SEM. The
relative quantification of genes was analyzed using standard $2^{-\Delta\Delta ct}$ method. For relative fold-change, the respective
expression value for the same gene from untreated plant leaf samples was taken as 1. Statistical significance was
obtained from one-way ANOVA using the Turkey's multiple comparison in the Prism version 7.0 software, and
were represented as *, $P \leq 0.05$, **, $P \leq 0.01$ and ***, $P \leq 0.001$.

293

294   *SEDOHEPTULOSE 1-7-BI-PHOSPHATE* (OsSBPase) (Suzuki et al., 2021, Feng et al., 2007) was significantly
295   down-regulated to 0.27-folds in CNP-treated samples compared to their controls (Figure 6B). These results
296   indicated that the input to the calvin cycle through the *OsSBPase* as well as the photosynthetic yield, as indicated
297   through *OsOEE1* (Heide et al 2004) transcript expression levels, were deteriorated in the CNP-treated plants
298   compared to the untreated plants. To confirm the microscopic observations of stomatal parameters in the CNP-
299   treated plants, genes related to stomatal size and frequency including *EPIDERMAL PATTERNING FACTOR-*
300   *LIKE 9* (*OsEPFL9*) and *SUCROSE NON-FERMENTING-1 RELATED PROTEIN KINASE 2* (*OsSNRK2*), were
301   studied for their transcript expression levels. *OsEPFL9* transcript expression level was found to be reduced to
302   ~0.31-folds in the CNP-treated samples compared to the controls (Figure 6C). *OsSNRK2* transcript expression
303   level in the CNP-treated plants was found to be reduced to nearly half (~0.55-fold) compared to their controls
304   (Figure 6D). To understand the molecular basis of the altered water relation parameters in the CNP-treated plants,
305   water use efficiency (WUE) related aquaporin gene *PLASMA MEMBRANE INTRINSIC PROTEIN 2-5* (*OsPIP2-*
306   *5*) transcript level was studied comparatively. *OsPIP2-5* transcript level was significantly increased to ~2.5-fold
307   in the CNP-treated seedlings compared to the controls (Figure 6E). To confirm the involvement of CNP in abiotic
308   stress response *PROTEIN PHOSPHATASE 51* (*OsPP51*) transcript level was studied in CNP-treated seedlings

309 compared to their controls. *OsPP51* level was up-regulated to ~5-folds in the CNP-treated samples (Table S1)
310 indicating improved abiotic stress compared to the controls.

Effect of different abiotic stresses in CNP-treated seedlings

312 Improved water relation parameters, bigger sized stomata and altered endogenous ABA content urged to study
313 the effect of different abiotic stresses in CNP-treated seedlings. To this end, various stresses (i.e., cold at 18°C,
314 high temperature at 35 °C, salinity stress and induced drought using PEG) were imposed in separate experiments
315 on seedlings with or without CNP in growth medium.
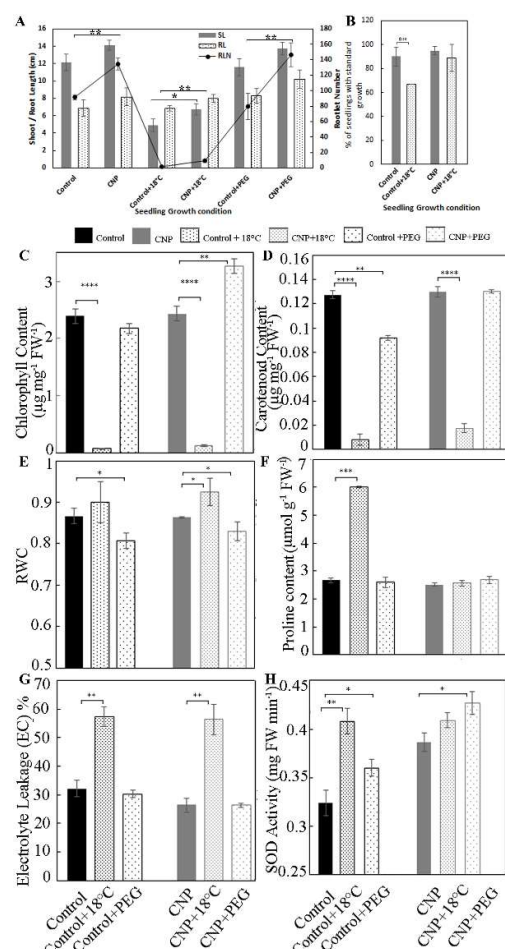
Figure 7. Effect of different abiotic stresses in CNP-treated seedlings. (A-B): Five-day-old seedlings were
318 carefully transferred on to medium containing PEG or salt and grown for 7 more days. On 13th – 14th day, seedling
319 growth parameters such as SL, RL, RLN were phenotyped. For cold treatment, seedlings were grown one more
320 day on MS medium before treatment for attaining higher growth to compensate the growth retardation due to cold.
321 All data presented were from minimum 30 seedlings in each experiment with 2 replications. (C-H): Physiological
322 and Biochemical characteristics of Cold and PEG stress response in CNP- treated seedlings. Physiological and
323 biochemical characteristics of seedlings with cold stress (18°C) or artificial drought due to PEG treatment for 7
324 days were assayed in 13d-old seedlings (14-day old in case of cold treatment). Seedlings were grown on MS or
325 CNP medium till initial 4d before stress treatment. C: Chlorophyll content, D: carotenoid content, E: RWC
326 content, F: proline content, G: Electrolyte leakage %, H: Superoxide dismutase activity. These experiments were
327 done thrice from leaves grown in at least 3 biological replicates. Data represented is a mean of 9 readings with 3
328 replications each time. Statistical significance was obtained from one-way ANOVA using the Turkey's multiple
329 comparison in the Prism version 7.0 software, and were represented as *, $P \le 0.05$, **, $P \le 0.01$ and
330 ***, $P \le 0.001$.

331   Changes in the RL under all these stresses were insignificant, hence, effects were studied in SL and RLN only.
332   Seedlings showed 16.5% increase in SL and ~47.1% increase in RLN due to CNP treatment (Figure. 7A). This
333   data served as the control for the abiotic stress treatments tested. Cold treatment for 7 d showed significant
334   decrease in SL and RLN (Figure. 7A). While SL decrease ~64% without CNP, it decreased ~60% with CNP due
335   to cold stress. RLN also showed higher decrease (~98%) without CNP and ~91.8% decrease with CNP due to
336   cold temperature. These results indicated that CNP treatment could partly rescue the drastic effects on seedling
337   growth during cold stress. PEG treatment creates osmotically induced drought environment at cellular level
338   (Purbajanti et al., 2019). PEG treatment showed marginal insignificant increase in SL in both untreated and CNP-
339   treated seedlings (Figure. 7A). Effect of PEG treatment showed significant contrasting response on RLN with or
340   without CNP, i.e., 12.7% decrease without CNP and 9.2% increase with CNP treatment as compared with the
341   control and CNP seedlings respectively. These results indicated that CNP treatment effectively counteracts the
342   PEG induced cellular drought to show increase in RLN. Salt stress induced decrease in SL, RL and RLN both
343   with and without CNP (data not shown). The % decrease due to salt stress was comparable, insignificant and
344   within the range. High temperature treatment resulted decrease in SL, RL and increase in RLN (data not shown),
345   however the differences were insignificant, therefore were not of interest. Despite germination, growth of
346   seedlings was hampered under low temperature from 6th d-14th d. But, CNP-treated seedlings SL showed less effect
347   as compared to the untreated ones (Figure.7B). These results indicated that CNP treatment has selective effects to
348   countereffect the stress caused due to cold temperature or PEG treatment.

349   **Countereffect of CNP-treatment on cold- and PEG-treatment induced stress in seedlings**

350   To ascertain the seedlings growth effects observed under cold-stress and PEG treatment and the countereffects of
351   CNP on it, various physiological and biochemical parameters were studied in 13 d-old (14 d-old in case of cold
352   stress) seedlings with or without CNP (Figure 7C-H). Cold stress resulted drastic decrease in chlorophyll content
353   (~32.8-fold and ~18.2-fold in case of control and CNP-treated seedlings respectively), with higher amount of chl
354   left in CNP-treated seedlings (Figure 7C). Similarly, carotenoid content was also drastically reduced due to cold
355   stress with ~16.1-fold and ~7.3-fold in case of control and CNP-treated seedlings respectively and lead to similar
356   pattern of higher carotenoid content in CNP-treated seedlings left after cold stress (Figure 7D). Relative water
357   content (RWC) was not significantly different in the control seedlings with or without cold stress, however it was
358   7.1% increased (p ≤ 0.05) in the CNP-treated seedlings with cold stress when compared to without cold stress
359   (Figure 7E). Electrolyte leakage (EC) % was significantly higher in the control as well as the CNP-treated
360   seedlings after cold stress (Figure 7G) (1.78-fold and 2.1-fold respectively). Proline accumulation showed
361   drastically different pattern among the CNP-treated and control seedlings (Figure 7F). In the control seedlings,
362   proline content was ~2.25-fold higher after cold stress as compared to the respective unstressed ones, whereas it
363   showed nearly no change in their values in CNP-treated seedlings due to cold stress. Reactive oxygen species
364   scavenging enzyme superoxide dismutase (SOD) activity was significantly higher in control (i.e., 5.7%), however
365   in the CNP-treated seedlings SOD activity was not much increased after cold stress (Figure 7H). These results
366   indicated that the effect of cold stress was alleviated due to CNP treatment seedlings with higher chlorophyll,
367   carotenoid, RWC, lesser SOD activity and nearly no more proline accumulation as compared to control seedlings.

368   PEG treatment for 6 d did not show significant decrease in chlorophyll in the control seedlings, whereas it showed
369   ~ 34.1% increase (p ≤ 0.01) in chlorophyll in CNP-treated seedlings (Figure 7C). Carotenoid content showed
370   significant decrease by 27.7% in the control seedlings due to PEG treatment, whereas it showed nearly no change
371   in the CNP-treated seedlings (Figure 7D). RWC decreased marginally but significantly in both control and CNP-
372   treated seedlings (6.8% and 3.8% respectively) after PEG treatment (Figure 7E). Proline accumulation (Figure
373   7F) and EC% (Figure 7G) were insignificant in both control and CNP-treated seedlings after PEG treatment.
374   Superoxide dismutase (SOD) enzyme activity was higher after PEG treatment in both control and CNP-treated
375   seedlings, however the CNP-treated seedlings it was higher than the control ones (Figure 7H). These results

376 indicated that after PEG treatment, CNP-treated seedlings retained drought resistance characteristics but only in
377 some parameters including chlorophyll, carotenoid content, RWC.

378 **Assessment of cold and drought stress tolerance in rice plants in reproductive stage**

379 To confirm the cold and PEG-induced-drought tolerance results obtained in the seedlings with CNP treatment,
380 cold and drought stress was imposed in rice plants in the reproductive stage (after 4th CNP treatment).

381
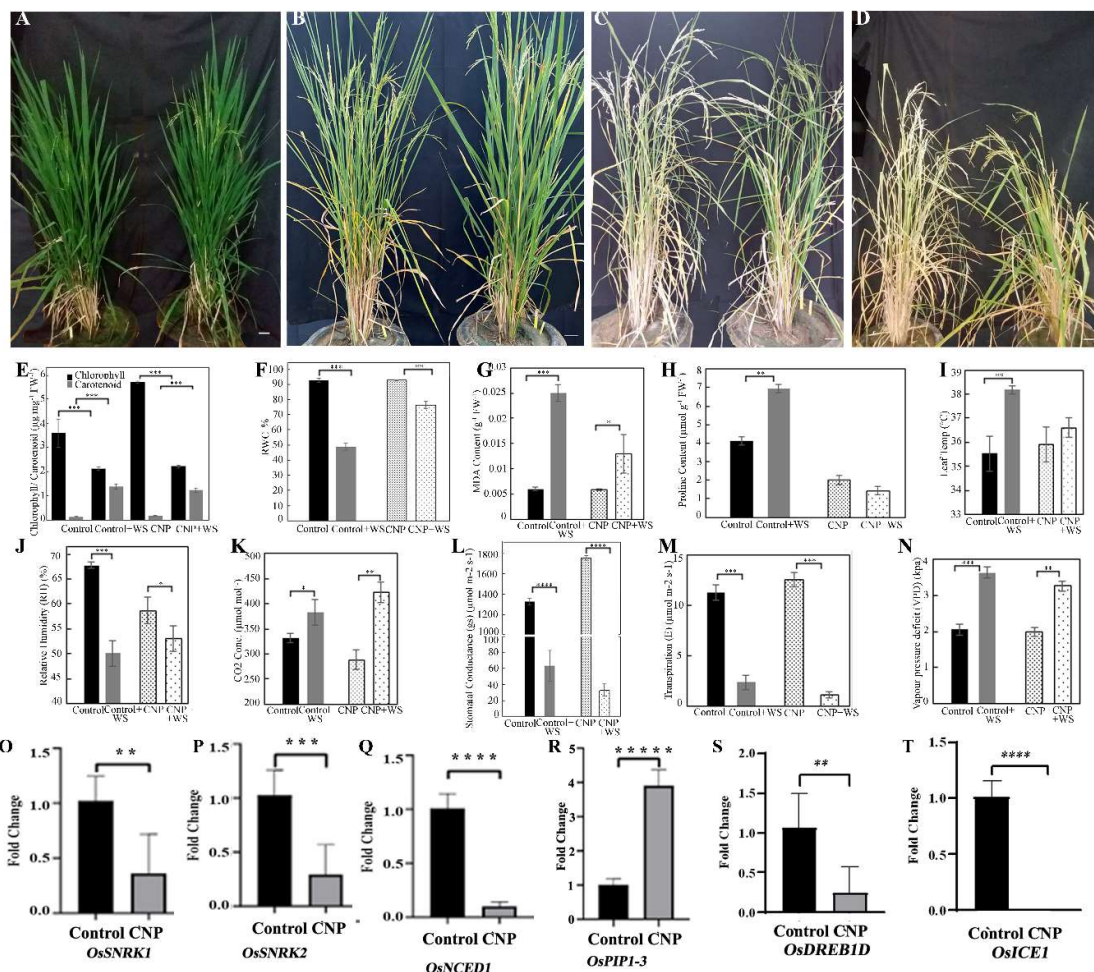
Figure 8. Effect of water stress in CNP-treated plants. (A-N): Water was withheld for 48 h after4th CNP
treatment and was compared with the untreated control plants. (A): Plants before water stress, Left plant is control
and right one is CNP-treated, (B)and (C): plants after 36- and 48-hours of water withheld respectively, (D): plants
after 24-hours of recovery from water stress. Physiological analyses such as (E) chlorophyll and carotenoid
content, (F) relative water content, (G) malondialdehyde content, (H) proline content, (I) leaf temperature, (J)
relative humidity, (K) leaf internal CO2 concentration, (L) stomatal conductance, (M) transpiration rate and
(N)vapor pressure deficit. were done from water-stresses leaf (top 2nd) samples. Data was obtained from 3
replicates each from 6 individual plants of untreated or CNP-treated plants. (O-T): Transcript expression analysis
in CNP-treated rice plant samples under cold or water stress. Transcript expression levels of genes involved in
ABA biosynthesis, ABA-regulated stomatal closure and cold tolerance, stomata and water relations were studied
using qRT-PCR in flag leaf samples after 48-hours of water stress. (O): *SUCROSE NON-FERMENTING-1*
RELATED PROTEIN KINASE 1 (*OsSNRK1*), (P): *SUCROSE NON-FERMENTING-1 RELATED PROTEIN*
KINASE 2 (*OsSNRK2*), (Q): *9-cis-EPOXYCAROTENOID DIOXYGENASE 1* (*OsNCED1*) (R) *PLASMA*
MEMBRANE INTRINSIC PROTEIN 1-3 (*OsPIP1-3*), (S) *DEHYDRATION RESPONSIVE ELEMENT BINDING*
PROTEIN 1D (*OsDREB1D*), (T): *INDUCER OF CBF EXPRESSION1* (*OsICE1*). Transcript levels of ACTIN

12

397 was used to normalise transcript levels. Reactions were done in triplicates from two biological replicates. Data
398 represents as the mean ±SEM. The relative quantification of genes was analyzed using standard $2^{-\Delta\Delta ct}$ method. For
399 relative fold-change, the respective expression value for the same gene from untreated plant leaf samples was
400 taken as 1. Statistical significance was obtained from one-way ANOVA using the Turkey's multiple comparison
401 in the Prism version 7.0 software, and were represented as *, $P \le 0.05$, **, $P \le 0.01$ and ***, $P \le 0.001$.

402 Cold stress at 10 °C for 10 d affected the cut leaves of untreated and CNP-treated leaves in a similar manner
403 (Suppl Figure 4). Yellowing of leaves, cold-induced lesions and drying progressed in similar fashion in untreated
404 and CNP-treated leaves (Suppl Figure 4A, 4B). Also, a recovery period of 24 h at room temperature was able to
405 regain the greenness of leaves in untreated and CNP-treated leaves in a similar manner (Suppl Figure 4C).
406 However, chlorophyll and carotenoid content in the cold-treated leaves were higher in the CNP-treated leaves
407 than the untreated ones (Suppl Figure 4D-E). Further parameters were not analyzed as the leaves of untreated and
408 CNP-treated leaves were apparently similar after cold stress.

409 Drought tolerance was tested by withholding water in control and CNP-treated pots (Figure 8A). Water-stress
410 (WS) for 36 h showed clearly resistant plant phenotype in the CNP-treated plants with greener stem, expanded
411 and greener leaves than the control plants (Figure 8B). After 48 h of water stress (Figure. 8C) and 24 h after re-
412 watering, the CNP-treated plants had clearly more greener leaves (Figure 8D). Chlorophyll content showed ~41%
413 and ~61.2% decrease in both the untreated and CNP-treated plants respectively after WS. However, CNP-treated
414 leaves retained the higher chlorophyll content after WS (Figure 8E). Carotenoid content showed to be increased
415 ~10 times after WS in both control and CNP-treated leaves with the later having the higher values after WS. RWC
416 decreased drastically to nearly half of its starting value in the control plants, however it retained 82% in CNP-
417 treated plants after WS (Figure 8F). MDA content sharply increased by ~ 4.2-fold of its initial value in the control
418 plants, however MDA content showed only ~2.2-fold increase in CNP-treated plants after WS (Figure 8G), thus
419 showing less MDA accumulation in CNP-treated plants than the control ones after WS. Proline accumulation
420 showed opposite pattern in control or CNP-treated plants after stress. While proline content increased to ~1.5-fold
421 in the control plants, it decreased non significantly in CNP-treated plants after WS (Figure 8H).

422 Water relation and related parameters also investigated in the CNP-treated plants in comparison with
423 control plants after WS. Leaf temperature increased by ~2.5°C in control while insignificantly in CNP-treated
424 plants after WS (Figure 8I). Relative humidity (RH) dropped ~37% in the control plants while it decreased
425 insignificantly in CNP-treated plants after WS (Figure 8J). Leaf CO_2 concentration increased only ~15% in control
426 plants, whereas in CNP-treated plants it increased to ~1.4 fold, maintaining the highest CO_2 concentration after
427 WS (Figure 8K). Stomatal conductance was higher in CNP-treated plants in well-watered conditions. WS lead to
428 drastic reduction of stomatal conductance in control plants up to ~20-fold. However, CNP-treated plants showed
429 even higher (~53-fold) reduction of stomatal conductance under WS conditions (Figure 8L). Transpiration rate
430 presented similar scenario like stomatal conductance showing drastic reduction after WS (Figure 8M). However,
431 the CNP-treated and untreated plants had insignificant differences in their transpiration rate values both before
432 and after WS. Vapor pressure deficit (VPD) was comparable between control and CNP-treated plants under well-
433 watered conditions, however, WS increased the VPD to nearly two-fold with insignificant differences between
434 control and CNP-treated plants after WS (Figure 8N). These results indicated that CNP treatment in the rice plants
435 could help to better withstand water stress by maintaining high chlorophyll carotenoid content, lower MDA,
436 proline content, lower leaf temperature and lower stomatal conductance, transpiration rate.

437 **Transcript expression analysis after water and cold stress in CNP-treated plants**

438 To confirm the drought and cold stress tolerance phenotype equipped with biochemical and physiological
439 characteristics in the CNP-treated plants during above stresses, transcript expressions of some ABA signaling,
440 stomatal parameters and aquaporin genes were studied from flag leaf samples of CNP-treated plants after cold or
441 water stress in comparison with their controls under well-watered condition (Figure 8O-8T). Expression levels of
442 ABA signaling components which are involved in stomatal closure such as *OsSNRK1* and *OsSNRK2* were down
443 to ~0.36 and ~0.29-folds respectively after water stress in the CNP-treated samples as compared to their controls
444 (Figure 8O, 8P). ABA biosynthesis gene *OsNCED1* expression was also down-regulated significantly by 10-fold
445 in the CNP-treated samples (Figure 8Q). Further, aquaporin gene *OsPIP1-3* expression was found to be
446 significantly up-regulated to ~3.9-folds in the CNP-treated samples as compared to their controls (Figure 8R).

13

447 These results indicated that CNP-treatment could alter ABA pathway, stomatal and water transport parameters to
448 withstand water stress. To validate the cold stress tolerance parameters with CNP treatment observed at the
449 seedlings stage and to access the cold tolerance at molecular level, transcript expression of *INDUCER OF CBF*
450 *EXPRESSION1 (OsICE1) (BHLH116)* and *DEHYDRATION RESPONSIVE ELEMENT BINDING PROTEIN 1D*
451 (*OsDREB1D)* were studied in rice flag leaf samples from CNP-treated and untreated plants after cold stress.
452 *OsICE1* expression was found to be significantly ($p<0.0005$) down-regulated to nearly zero in the CNP-treated
453 samples (Figure 8S). *OsDREB1D* was also significantly ($p<0.01$) down-regulated in the CNP-treated samples,
454 however the down-regulation was 0.25-folds as that of the controls (Figure 8T). These results confirmed that cold
455 tolerances response genes were down-regulated in the CNP-treated leaf samples.

Discussion

457 External exposure of carbon nanoparticle in the growth medium or pot soil of *Arabidopsis* (Kumar et al., 2108)
458 and rice (Panigrahy et al., 2021) respectively resulted some synergistic while some differential responses in our
459 two previous reports. In *Arabidopsis* it acted as a flowering time accelerator with photoperiod dependency, while
460 in rice it resulted improvement in growth and yield. The synergistic effects included involvement of red-light
461 photoreceptor Phytochrome B with shade avoidance like scenario in both the model plants. The present study not
462 only finds the causes of differential responses due to CNP to some extent in *At* and rice, but also it defines the
463 specific constraints of its use in rice plants and highlights its agronomic beneficial effects with respect to abiotic
464 stress tolerance in rice. For this purpose, several physiological, biochemical, microscopic analyses including
465 genomic analyses were accessed in both the model plant systems. CNP concentrations at 500 μg/mL -750 μg/mL
466 were found to be the optimum dosages showing best seedling growth among the 7 different concentrations tested
467 in the range between 200 μg/mL – 1500 μg/mL with rootlet number being the best parameter to study the seedling
468 response. Results of CNP and water uptake revealed that perimeter of xylem had an important role in water
469 uptake. Endocytosis inhibitor could not affect water uptake in the control seedlings. However, it could
470 reduce the water uptake when CNP was present the medium. Thus, CNP-coupled to water uptake was
471 endocytosis mediated. However, CNP aggregate was not affected with or without nocodazole. CNP
472 alone could be taken up using pinocytosis or energy consuming processes which requires further study.

473 CNP exposure induced specific resistance to cold stress tolerance at seedling stage with most of the physiological
474 and biochemical parameters according to cold tolerant response. However, in mature rice plant leaves cold
475 tolerance as not very prominent in rice leaf assay. Thought nearly half of the genes in rice microarray were up-
476 regulated, most of the transcripts cold stress response pathway were down regulated in *Arabidopsis*. Cold
477 tolerance response was exhibited in rice seedlings with CNP-treatment as verified through their SL and
478 biochemical parameters including Chl, carotenoid MDA and EC. However, the yellowing and cold-induced
479 lesions in the flag leaves due to cold treatment progressed in a similar manner in the CNP-treated as well as
480 untreated samples. The higher Chl content in the cold-stressed leaves could be due to the chl degradation
481 metabolites. Overexpression of rice *DEHYDRATION RESPONSIVE ELEMENT BINDING 1D* (*OsDREB1D*) or
482 *INDUCER OF CBF EXPRESSION 1* (*OsICE1*) showed cold stress tolerance (Zhang et al., 2009; Dian-jun et al.,
483 2008) in previous reports. Transcript expression of cold pathway genes (*OsICE1, OsDREB1D*) in our study
484 showed down-regulation, indicated that albeit the cold stress tolerance that was exhibited in the seedlings stage,
485 CNP-induced cold stress tolerance was not efficient enough to be exhibited in reproductive stage. Our previous
486 report of CNP treatment in rice resulted a clue of involvement of jasmonic acid and auxin pathway genes for CNP
487 response (Panigrahy et al., 2021). This indication of JA and auxin involvement was proved in the present study
488 by the highly elevated JA content in rice leaf samples (Suppl Figure 2) and also by the major involvement of the
489 auxin pathway gene in the genomic data of *At* and rice. The discrepancies in the CNP responses among the *At* and
490 rice could be due to the differential involvement of ABA pathway, photosynthesis and carbon metabolism pathway
491 genes among the two model plants. Nevertheless, almost all the Protein phosphatase 2C (PP2C) found in the
492 microarray data were up-regulated could clearly indicate strong positive involvement of ABA pathway for CNP
493 phenotype in rice. Sedoheptulose-1,7-Bisphosphatase (OsSBPase) is known as an important rate limiting enzyme
494 for fuelling carbon input to the calvin cycle (Feng et al., 2007) and the Oxygen Evolving Enhancer protein 1
495 (OEE1) of photosystem II is known to control the photosynthesis rate by being involved in ROS scavenging and
496 repair of PSII subunits (Heide et al., 2004). Presently, the decreased expression levels of these photosynthesis
497 genes indicated that the input to the calvin cycle (i.e. SBPase) as well as the yield of the light reaction (OEE1)

14

498   was less in CNP-treated plants despite higher carbon assimilation rate (Figure 2). However, the CNP-treated plants
499   exhibited an increase in yield/plant as shown previously. This could be due their higher expression of deposition
500   in the grain, higher rate of grain filling as shown before (Panigrahy et al., 2021). These observations were
501   supported by the elevated expression of *SOLUBLE STARCH SYNTHASE IIA* (*OsSSIIa*) and *SOLUBLE STARCH*
502   *SYNTHASE IIIA* (*OsSSIIIa*) (Table S1). Compensation to the photosynthetic calvin cycle could be provided by
503   the RuBisCO subunit binding-protein (*OsRBCS1*), which was highly over-expressed in the CNP-treated plants
504   (Table S1). Congruently, *Arabidopsis* photosynthesis and carbohydrate pathway showed majority of the genes up-
505   regulated (Table S2). These results explained the higher yields in the CNP-treated plants.

506   CNP-treated plants were found to have increased ABA content supported by increased expressions of ABA
507   biosynthesis gene in *Arabidopsis* (*AtNCED6*) and decreased expression (*OsNCED1*) in rice. *OsNCED1* expression
508   was shown to be down-regulated during water-stress and in turn stimulate ABA accumulation in rice through a
509   probable feedback inhibition (Changan et al., 2018). *Arabidopsis AtNCED6* expression was shown to increase
510   during water stress (Seiler et al., 2014). Hence, our results of increased ABA content were due to increased ABA
511   biosynthesis in *Arabidopsis* and feedback regulation due to *OsNCED1* in rice. Pyrabactin resistance 1 like (PYL)
512   genes are known to be the ABA receptor. Out of the 3 *PYL* genes found in rice microarray data, 2 of them were
513   up-regulated mildly in microarray data. Despite the two *PYL* genes found in *Arabidopsis* and one rice PYL genes
514   being down-regulated, the positive involvement of ABA pathway could be suggested due to the existence of nearly
515   13 *PYL* genes in rice (Miao et al., 2018) and 14 *PYL* genes in *Arabidopsis* (Gonzalez-Guzman et al., 2012), which
516   are presently not detected our experiment. Promoting root hair growth is characteristic effect of ABA in rice (Chen
517   et al., 2006). CNP-treated seedlings had higher number of rootlets and CNP-treated adult plants had larger root
518   volume (Panigrahy et al., 2021), it indicated that these effects could be due to elevated ABA content due to CNP.
519   To support this hypothesis, we observed no rootlets in CNP-treated seedlings while having increase in RLN in the
520   untreated seedlings with ABA treatment. It could be further inferenced that higher ABA content in CNP-treated
521   plants could result improved water relation parameters including higher stomata size, stomatal conductance and
522   WUE. Sucrose non-fermenting 1-related kinase 2 (OsSNRK2) is a key mediator regulating plant abiotic stress
523   and is involved in stomata closure (Kulik et al., 2011; Dey et al., 2016). OsSNRK2 is known to be a negative
524   regulator of ABA signaling. Epidermal patterning factor-like 9 (OsEPFL9) is known to be involved in stomatal
525   development and frequency (Yin et al., 2017). Protein phosphatase OsPP51 is known to modulate abiotic stress
526   response in rice (Singh et al., 2010). Aquaporins are the major determinants of water use efficiency in rice (Guo
527   et al., 2006). Our observations of improved water relation parameters were also backed by the increased expression
528   of stomata frequency gene *OSEPFL9*, *OsPP51* and aquaporin gene *OsPIP2-5* and decreased expression of
529   *OsSNRK2*. Hence, there are stronger evidence of improved water use efficiency in the CNP-treated plants. The
530   CNP-treated plants had better tolerance to water stress as evidenced by their increased RH, VPD and RWC
531   compared to the controls. CNP-treated plants could better withstand water stress also had faster recovery than
532   untreated plants, as evidenced not only from their phenotype but also from the several physiological parameters
533   including higher chlorophyll, carotenoids, proline content. Despite higher MDA content, CNP-treated plants had
534   advantage due to their higher water withholding capacity as evidenced by higher VPD, RH and reduced stomatal
535   conductance and reduced transpiration. These observations were also supported by the increased expression level
536   of *OsPIP1-3* responsible for water balance during drought (Verma et al., 2020). During water stress, ABA
537   signaling mediator controlling stomatal closure *OsSNRK1, OsSNRK2* and ABA biosynthesis gene *OsNCED1*
538   expressions were down indicating up-regulation of ABA pathway which may boost the water stress tolerance of
539   the CNP-treated plants.

540   There was an interference of CNP with the internal CO_2 concentration in CNP-treated plants which was observed
541   as reduced Ci in well-watered and increased Ci during water-stress as compared to their controls. It was shown in
542   previous report that carbon nanomaterials in plants can interfere with availability of carbon pool to the
543   photosynthesis. SWNT have been shown to add to the light capture and thereby add to the electron transfer and
544   increase photosynthesis rate (Khatri et al., 2018; Giraldo et al., 2014). Though the CNP could not add to the
545   photosynthetic carbon input in our study, somewhat similar phenomenon may interplay in CNP-treated plants to
546   have the present set of observations of improved WUE. Similar findings of carbon nanomaterials in ameliorating
547   plant water status by adjustment of osmolytes, reduced transpiration by stomatal closure due to abscisic acid
548   signaling with reduced photosynthesis have been discussed (Maswada et al., 2020).

549   In the present scenario, CNP, due to their black color, helped to hike the plant temperature in the rice
550   plants by absorbing more heat energy. Due to slightly warmer temperature, down-regulation of *PHYB*, the recently

15

551 known thermo-sensor, created a SAR-like syndrome of growth (Panigrahy et al., 2021). PhyB is known to regulate
552 stomatal density, transpiration rate and drought tolerance negatively in rice, as *OsphyB* mutants exhibited reduced
553 stomatal density with drought tolerance (Liu et al., 2011). The decreased *PhyB* expression levels in our case may
554 help to decrease the stomata density and increase their size by up-regulating the *OsEPFL9* expression levels. PhyB
555 was also shown to maintain the low ABA levels in well-watered as well as high ABA levels under water stress,
556 there by regulating the stomatal closure and stomatal conductance (Gonzalez et al., 2012). In Arabidopsis *AtphyB*
557 mutants exhibited increased stomatal conductance thereby less tolerant to water stress than the wild type
558 counterparts. Here it is worth mentioning that *phyB* mutants in rice or *Arabidopsis* resulted contrasting responses
559 to drought, and hence, further investigations are required to deduce conclusions of this contrasting response to
560 drought. With reduced *PHYB* levels in our case, the CNP-treated plants could show drought tolerance due to
561 reduced stomatal conductance, transpiration, lowering leaf temperature, maintaining VPD and RH. This could be
562 explained due to the property of carbon nanoparticles, by which they can act as hydroscopic binders of the
563 intracellular water and help plant cells to hold extra water in different compartments of cell (Ahmad et al., 2020).
564 With enlarged stomata, expression of aquaporin *OsPIP2-5* may be altered and may lead to increase the water
565 uptake. These changes may bring significant improvement with reduced transpiration and stomatal conductance
566 to exhibit water stress tolerance. Further investigations to demonstrate the hydroscopic abilities of CNP in our
567 case can unravel detailed molecular mechanisms underlaying the phenomenon of water stress tolerance in CNP-
568 treated plants. These results of this study is definitely a robust increment in building the fundamentals of nano
569 agriculture, the concept and applicability can be exploited in rice and other crops.

Materials and methods

Seedling and Plant growth condition

Seedling growth condition

573 Rice variety Swarna (MTU7029) was used for all experiments in this study. Swarna MTU7029 variety was
574 developed by All India Coordinated Rice Improvement Project (AICRIP) centre, Andhra Pradesh Rice Research
575 Institute (APRRI) and Regional Agricultural Research Station (RARS) Maruteru, Acharya NG Ranga Agricultural
576 University (ANGRAU), Andhra Pradesh, India in 1982 under the IET 5656 (IIRR, 2015; MARUTERU). Seeds
577 were surface-sterilized, stratified at 4 ºC for 2 d in dark and sown on 50 ml sterile Murashige and Skoog (MS)
578 media without or with carbon nanoparticle (CNP) in tissue culture containers. Further, seedlings were grown in
579 short-day cycles (i.e., 8 h day and 16 h night) under white light for 7 d. The white light was obtained from Philips17
580 W F17T8/TL741 USA Alto II technology tubes fitted in plant growth chambers (Model-AR36, Percival, USA).
581 Medium plates without CNP served as the controls. The intensity of incident white light was 80 µmol m^{-2} s^{-1}.
582 Seedling phenotype such as shoot length (SL), root length (RL), rootlet number (RLN) and nodal roots (NR) were
583 recorded on 8th day. Data presented the average of at least 2 biological replicates, and each biological replicate
584 was a mean of at least 30 measurements.

Plant growth condition

586 For carbon nanoparticle (CNP) treatment in rice plants, growth conditions were adherent to as done in Panigrahy
587 et al., (2021). Briefly, seedlings were grown on filter paper for 10 days, followed by growth on pooled pot up to
588 one more month. The 40-day old seedlings were transferred to single plant per pot. CNP treatments (500 µg/ml)
589 were added on the pot soil in every 15 days, i.e., on 45th, 60th, 75th, 90th day.

Abiotic stress treatments in rice seedlings

591 For imposing abiotic stress in seedling stage, rice seeds were de-husked and sterilized, followingly sown on 50
592 ml MS or CNP medium till 4 d before stress treatment. Cold and high temperature stresses were imposed at 18
593 °C and 35°C respectively. For PEG treatment, drought was induced with 10 % of PEG 6000 (Himedia, Cat #:
594 GRM401, CAS #: 25322-68-3) at pH 5.7. For salt stress assay, 150 mM NaCl (Himedia, Cat #: MB023, CAS #:
595 7647-14-5) containing MS media were prepared with pH 5.7. For ABA treatment, 2-cis 4-trans-abscisic acid
596 (Sigma, Cat # 862169) at 10µM was prepared in ethanol and sterile filtrated with 0.2 µm filter. It was mixed in
597 the autoclaved medium just before pouring (lukewarm) in tissue culture containers. Five-d-old seedlings were

598 carefully transferred on to medium containing PEG or salt or ABA plantons. For PEG, salt and high temperature,
599 seedlings were grown for 7 more days before they were phenotyped for the growth parameters such as SL, RL,
600 RLN on 13th day. For cold treatment, seedlings were grown for one more day on MS medium (5d) before treatment
601 for attaining higher growth to compensate the growth retardation due to cold. Hence, for cold and ABA treatment,
602 phenotyping was done on 14th day.

Cold or drought stress treatment in rice plants

604 Cold stress tolerance at 10 °C and drought stress tolerance was experimented in rice plants after four doses of
605 CNP treatment in the reproductive stage. For imposing cold stress, top second leaves from 6 plants were incubated
606 in water at 10 °C for nearly 10 d and observed for any leaf yellowing or deteriorating signs. Recovery from cold
607 stress was done by keeping the cold-stressed leaves in room temperature for 24 h. Chlorophyll and carotenoid
608 content was estimated from both the cold-stressed and recovery treated leaves. For drought treatment, water was
609 withheld for 48 h and recovery assay was done 24 h after re-watering. Physiological analyses such as chlorophyll
610 and carotenoid content, relative water content, malondialdehyde content, proline content, leaf temperature,
611 relative humidity, leaf internal CO_2 concentration, stomatal conductance, transpiration rate and vapor pressure
612 deficit. were done from water-stresses leaf (top 2nd) samples in comparison with their respective control leaf
613 samples. Data was obtained from 3 replicates each from 6 individual plants of untreated or CNP-treated plants.

Water relation Parameters assessment

615 Leaf gaseous exchange and water relation parameters were measured using a CIRAS-3 Portable Photosynthesis
616 System, Version 2.02, PP Systems, Amesbury, USA with parameter settings for PCL3 Universal Leaf Cuvette, 7
617 × 25 mm window. Settings for measurement were fixed with cuvette flow 300 CC min^{-1}, analyser flow 100CC
618 mm^{-1}, H_2O reference 80%, temperature sensor measurement IR sensor, Leaf area 1.75 cm, boundary layer
619 resistance 0.4 m^2 s mol^{-1} and stomatal ratio 50%. Physiological parameters such as leaf temperature (Tleaf),
620 relative humidity (RH), photosynthetically active radiation inside leaf (PARi), Assimilation (A_n), stomatal
621 conductance (gs), transpiration rate (E), vapour pressure density (VPD), internal carbon concentration (Ci) and
622 water use efficiency (WUE) were recorded in control and CNP-treated plants in the middle part of top 2nd leaf.
623 The recordings were done before each CNP treatment and finally 15 days after (on the 125th day) the last treatment.
624 Hence, 45th, 60th, 75th, 90th, 125th day measurements were noted as 0-day, 15th-day, 30th -day, 45th -day and 60th -
625 day of CNP-treatment respectively. Each data point is a mean of 108 recordings with 6 plants from each either
626 untreated or CNP-treated plants. For each plant 18 recordings were done from 3 leaves in time series of 5 seconds
627 interval, with 6 readings from each leaf.

Tissue fixation and histological analysis using Confocal Microscopy

629 For stomata visualization in leaf tissue, samples from 9 d-old seedlings or 90 d-old plants (after 4th CNP treatment)
630 were fixed with FAA substituted with methanol (45% methanol, 10% formaldehyde, 5% Glacial acetic acid and
631 40% distilled water) under vacuum using a portable vacuum pump for 15-20 minutes. Leaf samples were stained
632 with propidium iodide in (1 :1000 v/v) phosphate buffer to visualise morphology of stomata. Tissues were
633 mounted in glycerol. For visualization of CNP aggregates protocol from Allen et al (1940) with slight
634 modification were followed. Briefly, seedling root tissues with or without CNP and / or nocodazole
635 were fixed with FAA with vacuum overnight. On second day, samples were washed with ethanol,
636 dipped in 0.1% eosin at 4°C. Next day, samples were washed with xylene wash series for 2 hrs, followed
637 by moulding in paraplast at 65°C. On 8th day, wax embedding was done at 4°C overnight. Sectioning
638 was done and sample ribbons were kept in water-bath at 50 °C. Deparaffinization was done with xylene
639 and ethanol. Mounting with glycerol was done after staining with safranin. A Leica SP8 confocal
640 microscope system operating on a DMI600 inverted microscope, equipped with 63× NA 1.3 glycerol
641 immersion lenses (Leica, Wetzlar, Germany), was used for imaging. High resolution Z stack images
642 (1,024 pixels square) were recorded with 4-fold line averaging and a 1.00 μm step size. Along with
643 concurrent transmitted light images, fluorescence images were collected from 420-500 nm using
644 excitation at 405 nm. All image series were captured with the same imaging conditions. Images were

17

modified using standard brightness and contrast settings in Photoshop (version CS4, Adobe Systems, San Jose, CA, USA) and ImageJ software.

Physiological and Biochemical analyses of CNP treatment in rice seedlings

For all the physiological and biochemical assays, the 14th d-old seedlings samples with or without cold treatment at 18 °C or 13th d-old seedlings leaf samples with or without PEG treatment were used. All physiological and biochemical parameters were done thrice with three replicates in each set. Data were generated from the mean and the SEM. Significant differences were determined using one-way ANOVA using the Turkey's multiple comparison in the Prism version 7.0 software. For Chlorophyll and carotenoid content, pigments were extracted in 80% acetone extract and estimated according to Arnon (1949) from the absorbances values at 663 nm, 647 nm and 480 nm (Panigrahy et al., 2018). Relative water content (RWC) was analysed using the formula, RWC = ((FW-DW) / (TW-DW)) × 100 Where: FW = Fresh weight; TW = turgid weight. Proline content was spectrophotometrically estimated at 520 nm according to Carillo et al. (2011), with little modification. Briefly, 20 mg leaf samples were extracted in 70% ethanol in 1:50 w/v proportion. Reaction mixture was prepared mixing 1% ninhydrin, 60% acetic acid, 20% ethanol. Leaf extracts were mixed with the reaction mixture (1:2 v/v), heated at 95°C for 10 min and supernatant was taken. For standard curve, L-proline (Hi-media, Cat # 147-85-3) was used. Malondialdehyde (MDA) content was determined according to Khan and Panda (2008) with little modifications. Briefly, 50 mg of leaf samples were ground with extraction buffer containing 0.25% thiobarbituric acid (TBA) and 10% trochloroacetic acid (TCA) followed by incubation at 95°C for 30 min. The extract was centrifuged at 10k for 10 min and absorbance of the supernatant was measured at 532 nm. Senthilkumar et al. (2021) For electrolyte leakage (EL) percentage, leaf samples were cut in to 0.3 cm × 1 cm pieces and prepared so as to have equal fresh weight with equal number of cuts. EL and were assayed according to Bajji et al. (2002) and (Flint et al. 1967)

Abscisic acid treatment

ABA at 10µM was prepared in ethanol and sterile filtrated. It was mixed in the autoclaved medium just before pouring (luke warm) in tissue culture containers. Dehusked and sterilized seeds were grown on MS medium till 4 d, after which they were trans with or without CNP and ABA separately.

Endocytosis inhibitor treatment

Seedlings were grown in water for 8 days and nocodazole treatment was done according to Chem et al. (2018), briefly, 10µM in ethanol in stock was applied on the 3rd day. Water uptake was estimated from the water left after 8 days. Water uptake/ seedling measured by subtracting seedling weight from the amount of water taken up. Root samples with or without inhibitor were processed for confocal microscopy.

Defence Hormone estimation in rice leaf samples

Hormone estimation was done in triplicates from ~100 mg leaf samples of rice plants after 4th CNP treatment on 90th d. Estimation of defence hormones including abscisic acid (ABA), salicylic acid (SA) and jasmonic acid (JA) were done according to Vadassery et al., (2012). Leaf tissues were lypholized overnight after grinding with the help of a tissue lyser (Tissuelyser II, Retsch, Qiagen). Standards used were 1 ml of methanol containing 40 ng ml^{-1} of D6-jasmonic acid, (HPC Standards GmbH, Cunners dorf, Germany), 40 ng ml^{-1} D4-salicylic acid, 40 ng ml^{-1} D6-abscisic acid, and 8 ng ml^{-1} of jasmonic acid- [13C6] isoleucine conjugate for JA, SA, ABA and oxylipins respectively. The lipholyzed samples were extracted in methanol. Analysis of the samples was done with Exion LC (Sciex ®) UHPLC system using 0.05% formic acid as mobile phase A and acetonitrile as mobile phase B. for separation, Zorbax Eclipse XDB-C 18 column (50 x 4.6 mm, 1.8 µm, Agilent) was used coupled with a triple Quadruple-trap MS/MS system (Sciex 6500+) in negative ionization mode. The flow rate was 1 ml min^{-1} and isocratic elution profile were: up to 0.5 min: 5% B; 0.5 - 9.5 min: 5 - 42% B; 9.5 - 9.51 min: 42 - 100% B; 9.51 - 12 min: 100% B and 12.1 – 15 min: 5% B. Scheduled Multiple-reaction monitoring (MRM) is used to observe

18

690   precisely analyte parent ion → product ion with detection window of 60 sec. Defense hormones were quantified
691   relatively to the signal of their corresponding internal standard's concentrations.

Abscisic acid quantification in rice seedling

693   Quantification of ABA from seedling samples was done according to Ali et al., (2011). Nearly 100 mg seedlings
694   were homogenized with 80 % methanol at 4 ºC. After filtering, samples were lyophilized with Heto DryWinner
695   CT/DW 60E and redissolved in 0.5M phosphate buffer (pH 8). The samples were further purified through
696   Sephadex G10 column and the eluted solution was lyophilized again. The residue was dissolved in acetonitrile
697   and further filtered by 0.45 µm membrane filter (Waters) for HPLC analysis. The partially purified samples were
698   analyzed using an HPLC system (Waters 1525 Binary HPLC) equipped with a photodiode-array (PDA) detector
699   (Waters 2998) and RP-C18 column (5 mm packing; 250 x 4.6 mm internal diameter (ID). Acetonitrile with 0.5%
700   acetic acid was used as a mobile phase and run isocratically with a flow rate of 0.3 ml min^{-1}. The sample was
701   injected with a SGE Analytical syringe (Melbourne, Australia) into the HPLC column through a Rheodyne (Oak
702   Harbor, USA) injection valve equipped with 100 ul sample loop. The detection wavelength was 254 nm. Standard
703   stock solution of pure ABA was prepared by dissolving 1 mg of ABA (Sigma, extra pure) in 1 ml of HPLC grade
704   acetonitrile. Quantification of ABA in the rice seedlings was carried out by comparing the standard curve
705   generated through Breeze 2 software of Waters HPLC.

RNA isolation and genome-wide transcript expression analysis

RNA isolation

708   Total RNA was isolated from rice flag leaves and *Arabidopsis* seedlings for genome-wide microarray analysis
709   and transcriptome analysis respectively. For microarray analysis, rice flag leaves from untreated or CNP-treated
710   plants were sampled after 4th CNP treatment on the day of complete emergence of the panicle from the main stem.
711   For transcriptome sequencing, 14 d-old *Arabidopsis thaliana* (*At*) Col-0 seedlings grown of MS or CNP medium
712   were harvested. All samples were sampled with liquid N_2 and Experiments were performed in duplicates. RNA
713   was extracted from ~200 mg frozen rice leaves or 1 g of *At* seedlings using Qiagen RNAeasy Plant Mini kit
714   (Cat#74904). Briefly, leaves were homogenized using TOMY smasher homogenizer with liquid N_2 and RLT
715   buffer. Lysate was centrifuged and supernatant was mixed with RW1 buffer and loaded onto Qiagen RNeasy
716   column and further steps including on-column DNase treatment (Qiagen RNase free DNase Cat#79254) were
717   followed as per manufacturer's guidelines. RNA was eluted in Nuclease free water (Cat#AM9938, Ambion,
718   USA). Quantity and purity of the RNA were evaluated using the Nanodrop 2000 Spectrophotometer
719   (ThermoFischer, USA) from 260/280 values. Integrity of RNA was verified on the 2100 Bioanalyzer (Agilent,
720   USA) using rRNA 28S/18S ratios and RNA integrity number (RIN).

Microarray experimentation and data analysis

722   The rice RNA samples for gene expression were labelled using Agilent Quick-Amp labelling Kit (p/n5190-0442).
723   The total RNA was reverse transcribed at 40°C using oligo dT primer tagged to a T7 polymerase promoter and
724   converted to double stranded cDNA. This cDNA was used as template for cRNA generation using in vitro
725   transcription and incorporation of the dye Cy3 CTP(Agilent). Cleaning of cRNA was done using Qiagen RNeasy
726   columns (Qiagen, Cat #: 74106) and quality assessed for yields and specific activity using the Nanodrop ND-
727   1000. Fragmentation (at 60 ºC) and hybridization (at 65º C for 16 hours) were done using the Gene Expression
728   Hybridization kit of (Agilent Technologies, In situ Hybridization kit, Part # 5190-0404). An Agilent Rice Gene
729   Expression Microarray 8x60k (AMADID 64722) was used for hybridization. Hybridization was carried out in
730   Agilent's Surehyb Chambers. Washing using Agilent Gene Expression wash buffers (Agilent Technologies, Part
731   # 5188-5327) and scanning was done using the Agilent Microarray Scanner (Agilent Technologies, Part Number
732   G2600D). Microarray data analysis was performed from the extracted raw data and was analyzed using Agilent
733   GeneSpring GX (Version14.5) software. Normalization was done in GeneSpring GX using the 75th percentile
734   shift method was adapted to obtain the fold change (FC). Significantly down or up regulation (differentially
735   expressed genes, DEG) were identified with a cut off range in the logbase$_2$ of FC at $\leq$ -0.6 and $\geq$ 0.6 respectively
736   in the test samples with respect to control sample. Statistical student T-test p-value among the replicates was
737   calculated based on volcano Plot Algorithm. Differentially regulated genes were clustered using hierarchical

738   clustering based on Pearson coefficient correlation algorithm to identify significant gene expression patterns. For
739   function and pathway analysis differentially expressed genes were validated using Biological Analysis tool
740   DAVID (http://david.abcc.ncifcrf.gov/).

741   **Transcriptome sequencing and data analysis**

742   *Arabidopsis thaliana* RNA sequencing libraries were prepared with Illumina-compatible NEBNext® Ultra™ II
743   Directional RNA Library Preparation Kit (New England BioLabs, MA, USA). Five hundred ng of total RNA was
744   taken for mRNA isolation. Fragmented and primed mRNA was further subjected to first strand synthesis followed
745   by second strand synthesis. The double stranded cDNA was purified using JetSeq magnetic beads (Bio, # 68031).
746   Purified cDNA was end-repaired on Illumina HiSeq X Ten sequencer (Illumina, San Diego, USA), adenylated
747   and ligated to Illumina adapters as per NEBNext® Ultra™ II. Sequencing libraries were purified with JetSeq
748   Beads. Illumina-compatible sequencing libraries were quantified by Qubit fluorometer (Thermo Fisher Scientific,
749   MA, USA) and fragment size distribution was analyzed on Agilent 2200 TapeStation. The Illumina libraries
750   showed average fragment size range of 433 bp which was sufficient concentration to get the sequencing data.
751   Transcriptome analysis was performed by processing the raw data for removal of low-quality data and adapter
752   sequences. The data obtained from the sequencing run was demultiplexed using Bcl2fastq software v2.20 and
753   FastQ files were generated based on the unique dual barcode sequences. The raw reads were processed using
754   FastQC2 (v0.11.8) software for quality assessment and pre-processing which includes removing the adapter
755   sequences and low-quality bases (<q30) using TrimGalore3.

756   Illumina sequencing generated a total of 65713,399 paired end raw data. Nearly 98.08% of total reads were
757   retained as high quality (>Q30) data. The pre-processed 16.1 million high-quality reads were considered for
758   alignment with reference *Arabidopsis thaliana* genome using a splice aligner using Hisat24 with the default
759   parameters to identify the alignment percentage and classified into aligned and unaligned reads. About 97.58% of
760   the reads were aligned to the reference genome. HTSeq5 was used to estimate and calculate gene abundance.
761   DESeq6 used the absolute counts for genes to identify and used for differential expression calculations. DEG were
762   categorized as Up, Down based on cut-off of $\log_2$fold change +/-1.0 value respectively. Genes were annotated
763   using homology approach to assign functional annotation using BLAST7 tool against "Viridiplantae" data from
764   the Uniprot database. The DEG were analysed for GO annotation and pathway analysis to understand the
765   functional role of each expressed gene. A match was found when e-value less than e^{-5} and minimum similarity
766   greater than 30%. Pathway analysis was done by using KAAS8 Server. Enrichment analysis for all up and down
767   regulated genes was performed using ShinyGO9 tool.

768   **Real-time PCR (Q-PCR) analysis**

769   For real-time PCR analysis, plants tissues (rice flag leaves and *Arabidopsis* seedlings) were sampled with liquid
770   N_2. The growth condition and sampling procedure of rice flag leaves for this purpose was similar to as that for the
771   microarray expression analysis (section). *Arabidopsis* seedlings (10 d-old) were sampled after 12 h of onset of
772   light in the long-day cycle (Zt-12). RNA was extracted from using RNeasy Plant Mini Kit Qiagen (Cat #74104)
773   and one µg of total RNA was used to obtain cDNA using Reverse Transcription Super-mix (Cat #1708840).
774   Quantitative RT-PCR (qRT-PCR) was carried out using the Bio-Rad laboratories' CFX384 Touch™ Real time
775   detection system and iTaq™ universal SYBR green super mix following the manufacturer's instructions as done
776   previously (Kumar et al., 2018). Primer Quest tool (Integrated DNA Technologies, Inc., USA) was used to design
777   gene-specific primers (Table S3). All reactions were carried out in hard shell 384-well PCR plates (Bio-Rad, Cat
778   #: HSP3805). ACTIN was used to normalise transcript levels. The qRT-PCR reactions were done in triplicates
779   from two biological replicates. Data represents as the mean ±SEM. The relative quantification of genes was
780   analyzed using standard $2^{-\Delta\Delta ct}$ as described by Pfaffl (2001). For relative fold-change, the respective expression
781   value for the same gene from untreated plant leaf samples was taken as 1.

782

783   # References

784   Ahmad, J., Qamar, S., Kausar, N. and Qureshi, M.I. Nanoparticles: the magic bullets in mitigating drought stress
785   in plants. *Nanobiotechnol. Agric.*, 145-161. (2020)

786 Allen, C.E., 1940. Plant Microtechnique: Plant Microtechnique. By Donald A. Johansen. xi+ 523 pp. New York:
787 $4.50. *Science*, *92*(2383), pp.200-201. (McGraw-Hill Book Company, 1940)

788 Alejandro P-de-L. Interaction of Nanomaterials with Plants: What Do We Need for Real Applications in
789 Agriculture? *Front Environ Sci.* **5,** 10.3389/fenvs.2017.00012 (2017)

790 Ali, H. M., Siddiqui, M. H., Al-Whaibi, M. H., Basalah, M. O., Sakran, A. M., & El-Zaidy, M. Effect of proline
791 and abscisic acid on the growth and physiological performance of faba bean under water stress. *Pak. J. Bot*, *45*(3),
792 933-940. (2013).

793 Ali, S., Mehmood, A. and Khan, N., Uptake, translocation, and consequences of nanomaterials on plant growth
794 and stress adaptation. *Journal of Nanomaterials*, *2021*. (2021)

795 An, J., Hu, P., Li, F., Wu, H., Shen, Y., White, J.C., Tian, X., Li, Z. and Giraldo, J.P., Emerging investigator
796 series: molecular mechanisms of plant salinity stress tolerance improvement by seed priming with cerium oxide
797 nanoparticles. *Environmental Science: Nano*, *7*(8), 2214-2228. (2020)

798 Bajji, Mohammed & Kinet, Jean-Marie. The use of the electrolyte leakage method for assessing cell membrane
799 stability as a water stress tolerance test in durum wheat. *Plant Growth Regulation*. **36,** 61-70.
800 10.1023/A:1014732714549. (2002).

801 Carillo, P. and Gibon, Y. Protocol: extraction and determination of proline. *PrometheusWiki*, 1-5. (2011)

802 Changan, S.S., Ali, K., Kumar, V. et al. Abscisic acid biosynthesis under water stress: anomalous behaviour of
803 the 9-cis-epoxycarotenoid dioxygenase1 (*NCED1*) gene in rice. *Biol Plant* **62,** 663–670.
804 https://doi.org/10.1007/s10535-018-0807-2 (2018)

805 Chen, C. W., Yang, Y. W., Lur, H. S., Tsai, Y. G., & Chang, M. C. A novel function of abscisic acid in the
806 regulation of rice (*Oryza sativa* L.) root growth and development. *Plant and Cell Physiology*, *47*(1), 1-13. (2006).

807 Chen, L., Wang, H., Xiang, L., Nie, C., Liang, T., Xie, F., et al. Highly hydrophilic carbon nanoparticles: uptake
808 mechanism by mammalian and plant cells. *RSC Adv.* **8**, 35246 (2018)

809 Deng, C., Wang, Y., Navarro, G., Sun, Y., Cota-Ruiz, K., Hernandez-Viezcas, J.A., Niu, G., Li, C., White, J.C.
810 and Gardea-Torresdey, J. Copper oxide (CuO) nanoparticles affect yield, nutritional quality, and auxin associated
811 gene expression in weedy and cultivated rice (*Oryza sativa* L.) grains. *Science of The Total
812 Environment*, **810,**152260. (2022)

813 Dey, A., Samanta, M.K., Gayen, S. *et al.* The sucrose non-fermenting 1-related kinase 2 gene *SAPK9* improves
814 drought tolerance and grain yield in rice by modulating cellular osmotic potential, stomatal closure and stress-
815 responsive gene expression. *BMC Plant Biol* **16**, 158. https://doi.org/10.1186/s12870-016-0845-x(2016)

816 Dian-jun, X.I.A.N.G., Xiang-yang, H.U., Yu, Z.H.A.N.G. and Kui-de, Y.I.N. Over-Expression of *ICE1* Gene in
817 Transgenic Rice Improves Cold Tolerance. *Rice Science* **15(3),** p.173. (2008)

818 Feng, L., Han, Y., Liu, G., An, B., Yang, J., Yang, G., Li, Y., & Zhu, Y. Overexpression of sedoheptulose-1,7-
819 bisphosphatase enhances photosynthesis and growth under salt stress in transgenic rice plants. *Functional Plant
820 Biology: FPB*, *34*(9), 822–834. (2007).

821 Flint H.L., Boyce B.R. and Beattie D.J. Index of injury – A useful expression of freezing injury to plant tissues as
822 deter-mined by the electrolytic method. Can. *J. Plant Sci.* **47,** 229–230. (1967)

823

824 Giraldo, J. P., Landry, M. P., Faltermeier, S. M., McNicholas, T. P., Iverson, N. M., Boghossian, A. A., & Strano,
825 M. SPlant nanobionics approach to augment photosynthesis and biochemical sensing. *Nature Materials, 13*(4),
826 400–408. (2014).

827 Gonzalez-Guzman, M., Pizzio, G. A., Antoni, R., Vera-Sirera, F., Merilo, E., Bassel, G. W., Fernández, M. A., et
828 al. *Arabidopsis* PYR/PYL/RCAR receptors play a major role in quantitative regulation of stomatal aperture and
829 transcriptional response to abscisic acid. *The Plant cell.* **24(6)**, 2483–2496.
830 https://doi.org/10.1105/tpc.112.098574 (2012).

831 Guo, L., Wang, Z., Lin, H. *et al.* Expression and functional analysis of the rice plasma-membrane intrinsic protein
832 gene family. *Cell Res* **16**, 277–286. https://doi.org/10.1038/sj.cr.731003 (2006)

833 Hatami, M., Hadian, J. and Ghorbanpour, M., Mechanisms underlying toxicity and stimulatory role of single-
834 walled carbon nanotubes in Hyoscyamus niger during drought stress simulated by polyethylene glycol. *Journal*
835 *of hazardous materials*, **324**, 306-320. (2017)

836 Heide, Heinrich & Kalisz, Henryk & Follmann, Hartmut. The oxygen evolving enhancer protein 1 (OEE) of
837 photosystem II in green algae exhibits thioredoxin activity. *Journal of plant physiology.* 161. 139-49.
838 10.1078/0176-1617-01033. (2004).

839 IIRR Newsletter, AICRIP Centre Profiles Andhra Pradesh Rice Research Institute & Regional Agricultural
840 Research Station, Maruteru. Angrau, Andhra Pradesh, 13(2): pp 2 (2015) IIRR NL Apr_June_2015.pdf (icar-
841 iirr.org)

842 Jha, S., Pudake, R.N. Molecular Mechanism of Plant–Nanoparticle Interactions. In: Kole, C., Kumar, D.,
843 Khodakovskaya, M. (eds) Plant Nanotechnology. Springer, Cham. https://doi.org/10.1007/978-3-319-42154-4_7
844 (2016).

845 Khan, M.H. and Panda, S.K., Alterations in root lipid peroxidation and antioxidative responses in two rice
846 cultivars under NaCl-salinity stress. *Acta Physiologiae Plantarum*, **30**(1), 81-89. (2008).

847 Khatri, K., Rathore, M. S. 'Plant Nanobionics and Its Applications for Developing Plants with Improved
848 Photosynthetic Capacity', in J. C. G. Cañedo, G. L. L. Lizárraga (eds.), Photosynthesis - From Its Evolution to
849 Future Improvements in Photosynthetic Efficiency Using Nanomaterials,. 10.5772/intechopen.76815.
850 (IntechOpen, London, 2018)

851 Kulik A, Wawer I, Krzywińska E, Bucholc M, Dobrowolska G. SnRK2 protein kinases--key regulators of plant
852 response to abiotic stresses. OMICS. **12**, 859-72. doi: 10.1089/omi.2011.0091. (2011)

853 Kumar A, Singh A, Panigrahy M, Sahoo P K, Panigrahi K C S. Carbon nanoparticles influence
854 photomorphogenesis and flowering time in *Arabidopsis thaliana*. *Plant Cell Rep*, **37**(6): 901-912. (2018)

855 Lahiani MH, Dervishi E, Chen J, Nima Z, Gaume A, Biris AS, Khodakovskaya MV (2013) Impact of carbon
856 nanotube exposure to seeds of valuable crops. *ACS Appl Mater Interf*. **5,**7965–7973

857 Liu, J., Zhang, F., Zhou, J., Chen, F. Wang, B., Xie, X. Phytochrome B control of total leaf area and stomatal
858 density affects drought tolerance in rice. *Plant Molecular Biology*. **78,** 289-300. 10.1007/s11103-011-9860-3.
859 (2011).

860 Majeed N, Panigrahi K C S, Sukla L B, John R, Panigrahy M. Application of carbon nanomaterials in plant
861 biotechnology. *Mater Today: Proc*, **30**(2), 340-345. (2020)

862 MARUTERU. AICRIP Intranet 01 Maruteru.pdf (aicrip-intranet.in)

863 Maswada, H.F., Mazrou, Y.S., Elzaawely, A.A. and Eldein, S.M.A., Nanomaterials. Effective tools for field and
864 horticultural crops to cope with drought stress: A review. *Spanish Journal of Agricultural Research*, **18(2)**, p.15.
865 (2020)

866 Miao, C., Xiao, L., Hua, K., Zou, C., Zhao, Y., Bressan, R.A. and Zhu, J.K., Mutations in a subfamily of abscisic
867 acid receptor genes promote rice growth and productivity. *Proc Nat Ac Sci*, **115(23)**, 6058-6063. (2018)

868 Panigrahy, M., Das, S., Poli, Y., Sahoo, P.K., Kumari, K. and Panigrahi, K.C., Carbon nanoparticle exerts positive
869 growth effects with increase in productivity by down-regulating phytochrome B and enhancing internal
870 temperature in rice. *Rice Science*, **28(3)**, 289-300. (2021)

871 Panigrahy, M., Sarla, N. and Panigrahi, K.C.S., Phenotypic, physiological and biochemical characterization of
872 rice introgression lines and mutants under prolonged shade condition. *Res. J. Life. Sci. Bioinform. Pharm. Chem.*
873 *Sci*, **4**, 115-131. (2018)

874 Pfaffl M W. A new mathematical model for relative quantification in real-time RT-PCR. *Nucl Acids Res*, **29 (9),**
875 e45. (2001)

876 Purbajanti, E. D., Kusmiyati, F., Fuskhah, E., Rosyida, R., Adinurani, P. G., & Vincēviča-Gaile, Z. Selection for
877 drought-resistant rice (*Oryza sativa* L.) using polyethylene glycol. In *IOP Conference Series: Earth and*
878 *Environmental Science* **293(1)** p. 012014). (2IOP Publishing. 019).

879 Rani, A, Kavita Rani, Jayanti Tokas, Anamika, Aastha Singh, Rakesh Kumar, Himani Punia & Sandeep Kumar. *et*
880 *al.* Nanomaterials for Agriculture Input Use Efficiency. In: Kumar, S., Meena, R.S., Jhariya, M.K. (eds)
881 Resources Use Efficiency in Agriculture. Springer, Singapore. https://doi.org/10.1007/978-981-15-6953-1_5
882 (2020).

883 Rico, C.M., Morales, M.I., Barrios, A.C., McCreary, R., Hong, J., Lee, W.Y., Nunez, J., Peralta-Videa, J.R. and
884 Gardea-Torresdey, J.L., Effect of cerium oxide nanoparticles on the quality of rice (Oryza sativa L.)
885 grains. *Journal of agricultural and food chemistry*, **61(47)**, 11278-11285. (2013)

886 Seiler, C., Harshavardhan, V. T., Reddy, P. S., Hensel, G., Kumlehn, J., Eschen-Lippold, L., Rajesh, K., Korzun,
887 V., Wobus, U., Lee, J., Selvaraj, G., & Sreenivasulu, N. Abscisic acid flux alterations result in differential abscisic
888 acid signaling responses and impact assimilation efficiency in barley under terminal drought stress. Plant
889 physiology, 164(4), 1677–1696. https://doi.org/10.1104/pp.113.229062 (2014).

890 Senthilkumar, M., Amaresan, N., Sankaranarayanan, A. Estimation of Malondialdehyde (MDA) by Thiobarbituric
891 Acid (TBA) Assay. In: Plant-Microbe Interactions. Springer Protocols Handbooks. Humana, New York, NY.
892 https://doi.org/10.1007/978-1-0716-1080-0_25 (2021).

893 Singh, A., Giri, J., Kapoor, S., Tyagi, A.K., Pandey, G.K. Protein phosphatase complement in rice: genome-wide
894 identification and transcriptional analysis under abiotic stress conditions and reproductive development. *BMC*
895 *Genomics*. **11,** 435. doi: 10.1186/1471-2164-11-435. (2010)

896 Suzuki, Y., Ishiyama, K., Cho, A., Takegahara-Tamakawa, Y., Wada, S., Miyake, C., Makino, A. Effects of co-
897 overproduction of Rubisco and chloroplast glyceraldehyde-3-phosphate dehydrogenase on photosynthesis in rice.
898 Soil Science and Plant Nutrition **67**:3, 283-287. (2021)

899 Vadassery, J., Reichelt, M., Hause, B., Gershenzon, J., Boland, W., Mithöfer, A. CML42-mediated calcium
900 signaling coordinates responses to Spodoptera herbivory and abiotic stresses in *Arabidopsis*, *Plant Physiology.*
901 **159,**1159–1175. https://doi.org/10.1104/pp.112.198150. (2012)

902 Yin, X., Biswal, A.K., Dionora, J. *et al.* CRISPR-Cas9 and CRISPR-Cpf1 mediated targeting of a stomatal
903 developmental gene *EPFL9* in rice. *Plant Cell Rep* **36**, 745–757. https://doi.org/10.1007/s00299-017-2118-z
904 (2017)

905 Zhang, Y., Chen, C., Jin, X.-F., Xiong, A.-S., Peng, R.-H., Hong, Y.-H., et al. Expression of a rice DREB1 gene,
906 OsDREB1D, enhances cold and high-salt tolerance in transgenic *Arabidopsis*. *BMB Reports*. Korean Society for
907 Biochemistry and Molecular Biology - BMB Reports. https://doi.org/10.5483/bmbrep.2009.**42.8.486** (2009)

908 Zhao, L., Lu, L., Wang, A., Zhang, H., Huang, M., Wu, H., Xing, B., Wang, Z. and Ji, R., Nano-biotechnology in
909 agriculture: use of nanomaterials to promote plant growth and stress tolerance. *Journal of Agricultural and Food*
910 *Chemistry*, **68(7)**, 1935-1947. (2020)

911 ## Acknowledgement

Authorship contribution statement

MP has designed the project, acquired funds. LM and JPK have done the experimental work. AK has done real-time PCR experiments. SM and JR have done the ABA content determination. GM has done the microscopy. KCP and GRR have acquired funds, provided infrastructural and institutional support, helped in designing, trouble shooting. All authors have read and agreed to the MS.

Data Availability

Microarray data sets for CNP treatment in rice plants can be accessed at: NCBI GEO Accession No: GSE200357, Title: "Effect of Carbon Nanoparticle Treatment in Rice Adult plants", https://www.ncbi.nlm.nih.gov/geo/query/acc.cgi?acc=GSE200357

Transcriptome sequencing data sets for CNP treatment in Arabidopsis seedlings can be accessed at NCBI SRA Submission Portal with the reviewer's link https://dataview.ncbi.nlm.nih.gov/object/PRJNA825704?reviewer=kefmtv4hfnnu7siae3kch7uekf

Competing Of Interests

The authors have no competing state of interests to disclose

Funding

937 **Supporting Information**

938
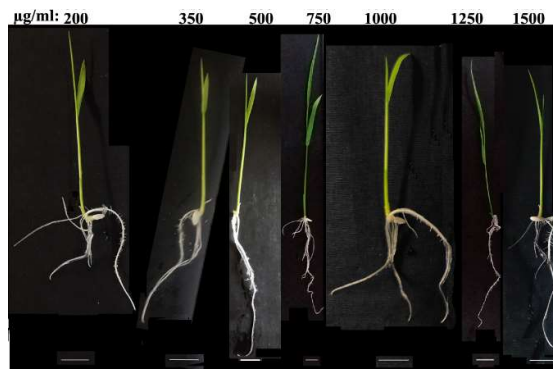
939 **Figure S1. Representative seedling pictures of dosage dependence effect of Carbon nanoparticle.** The
940 concentration of CNP in µg ml^{-1} is indicated on the top of each seedlings. Scale bar: 2 cm

941
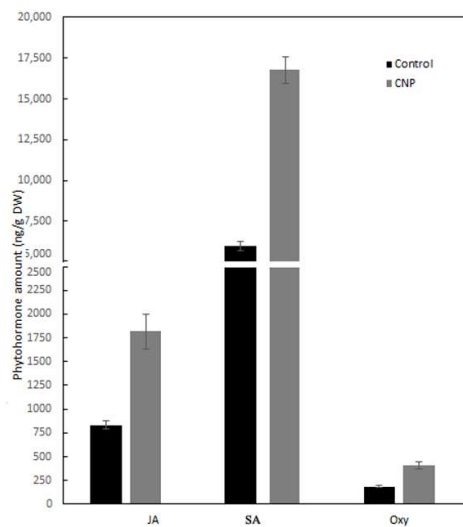
942 **Figure S2. Endogenous defence hormone quantification in CNP treated seedlings.** Defence hormones
943 including Jasmonic acid (JA), Salicylic acid (SA) and Oxylipins (Oxy) were quantified in adult leaf samples after
944 4th CNP treatment. Top second leaf was used for lyophilization and processed as explained in the section 2.6.1.
945 Data represented is a mean of three replicative measurements. Statistical significance was obtained from one-way
946 ANOVA using the Turkey's multiple comparison in the Prism version 7.0 software, and were represented as
947 *, $P \leq 0.05$, **, $P \leq 0.01$ and ***, $P \leq 0.001$.

25

948
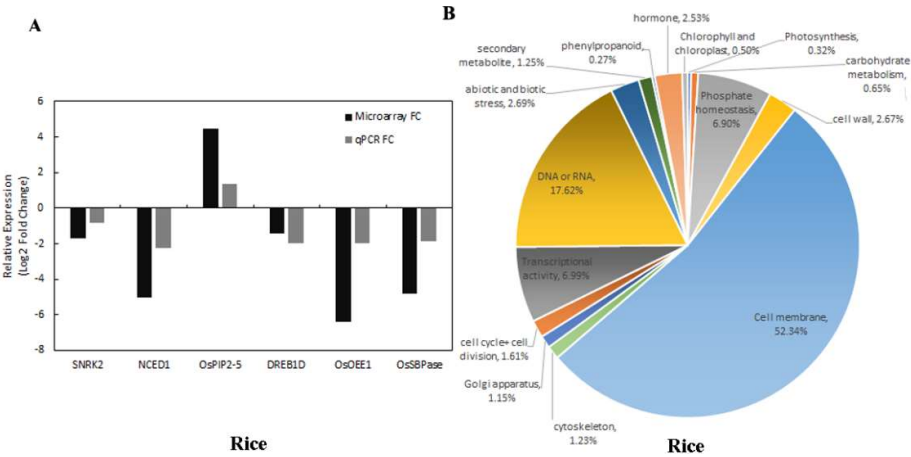
Figure S3. Function & pathway analysis and validation of microarray expression data from CNP-treated and control leaf samples. (A): Correlation plot among replicates of control and CNP-treatment samples (B) Differentially expressed genes (DEGs) obtained from microarray expression analysis were categorized according to their transcript details obtained from Rice Annotation Project (RAP-DB), MSU and CGSNL Databases. Functional details were obtained from GO annotations, KEGG database, UNIPROT and Oryzabase database. Pathway categorization was done according to the biological process, cellular category and molecular function. Percentage was obtained by calculating from total number of DEGs. (C): collinearity of the Log_2 fold change values obtained from microarray expression analysis and qPCR.

957
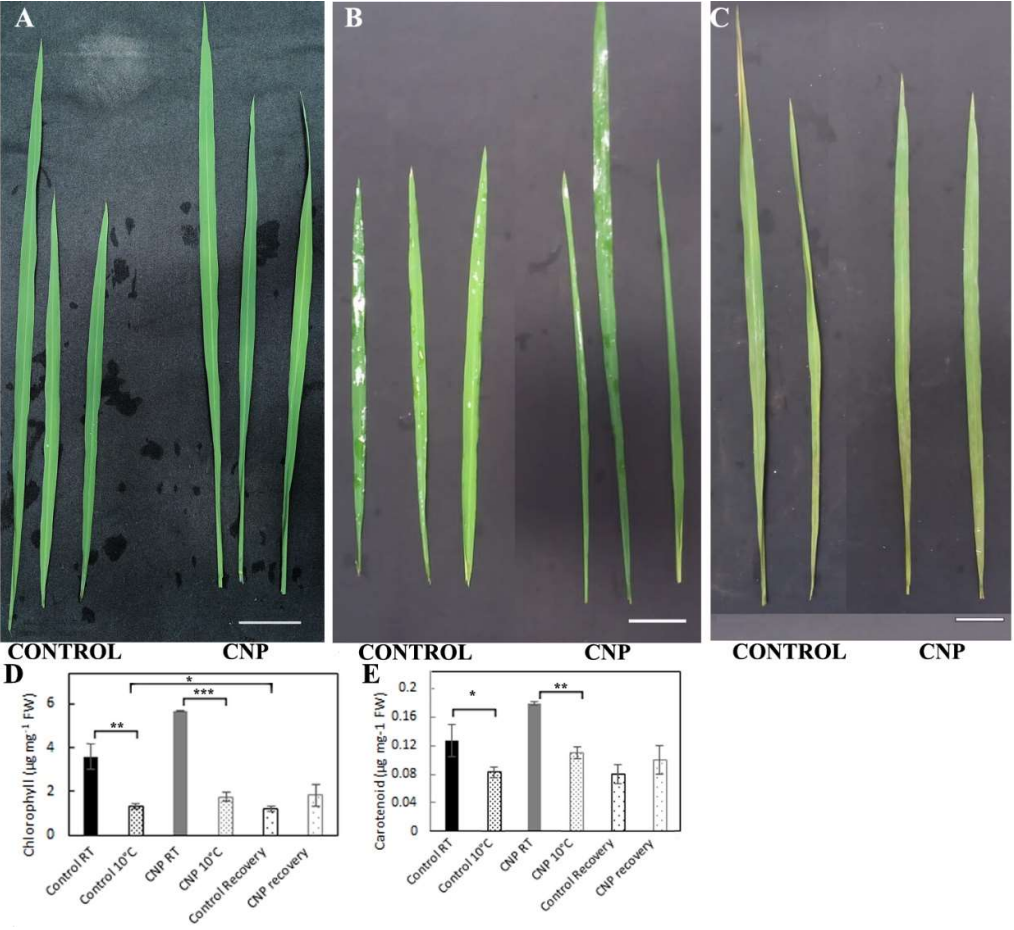
Figure S4. Cold treatment assay in flag leaves of CNP-treated and control plants. Cold stress was imposed in top second leaves taken from rice plants in the reproductive stage (after 4th CNP treatment). They were floated in equal amount of water and incubated in white light at 10°C for 10 days. (A) Leaves before cold stress (B) Leaves after cold stress (C) Leaves from cold stress were incubated for 24 h recovery at room temperature. (D) chlorophyll (E) carotenoid content were estimated from control and CNP-treated leaves mentioned above. The experiment was done thrice from leaves of 3 biological replicates. Statistical significance was obtained from one-way ANOVA using the Turkey's multiple comparison in the Prism version 7.0 software, and were represented as *, $P \leq 0.05$, **, $P \leq 0.01$ and ***, $P \leq 0.001$.

Table S1. Expression level of Transcripts of some selected pathway from microarray analysis in rice. Flag leaves on the day of final emergence of the panicle from the CNP treated and untreated plant were sampled with liquid N2 after 4th CNP treatment. Microarray analysis was done from two biological replicates each category. Normalization and Fold change was calculated as described in the materials and methods section. Transcript details are taken from Rice Annotation Project Database (RAP-DB). Pathway analysis was done using GO Ontology, KEGG and Biological Analysis tool DAVID (http://david.abcc.ncifcrf.gov/)

Table S1. Expression	Gene ID (RAP-DB)	FC (<+>	P-value	Gene Symbol	Gene Name
ABA pathway	Os06t0211200-02	2.06	0.02	OsAREB8, BZIP46	ABA-responsive element binding protein 1
	Os06t0211200-01	2.32	0.03	OsABL1	bZIP transcription factor 46, ABI5-like1
	Os08t0467500-02	3.65	0.03	OsEnS-122, A22	Abscisic acid and stress inducible (A22) gene
	Os10t0573400-01	1.66	0.00	RCAR10, OsPYL10	PYRABACTIN RESISTANCE 1 LIKE
	Os05t0473000-01	0.93	0.08	OsPYL6	PYRABACTIN RESISTANCE 1 LIKE
	Os02t0255500-01	-1.07	0.20	OsPYL10, RCAR3	PYRABACTIN RESISTANCE 1 LIKE
	Os05t0381400-01	2.13	0.30	OsPM19L1	AWPM-19-like protein 1
	Os02t0285300-01	9.76	0.01	OsDREPP2	developmentally regulated plasma membrane polypeptide 2
	Os11t0109000-01	5.33	0.03	OsPP116	protein phosphatase 2C73
	Os03t0301700-01	5.08	0.01	OsPP51	protein phosphatase 2C33
	Os05t0555100-01	3.26	0.01	OsB'kappa	PROTEIN PHOSPHATASE 2A REGULATORY SUBUNIT B' KAPPA
	Os09t0459600-01	3.13	0.11	OsPP109	protein phosphatase 2C69
	Os05t0572700-02	2.89	0.07	OsABI1	protein phosphatase 2C14
	Os04t0167900-00	2.48	0.02	OsPP61	protein phosphatase 2C37
	Os01t0656200-01	1.21	0.20	OsPP12	protein phosphatase 2C08
	Os02t0471500-02	1.10	0.00	OsPP24	protein phosphatase 2C14
	Os02t0606900-01	1.05	0.23	OsPP31	protein phosphatase 2C21
	Os03t0832400-01	0.99	0.07	OsPP60	protein phosphatase 2C36
	Os02t0471500-03	0.94	0.05	OsPP24	protein phosphatase 2C14
	Os02t0685600-01	0.88	0.04	OsPP36	protein phosphatase 2C25
	Os02t0471500-01	0.87	0.04	OsPP24	protein phosphatase 2C14
	Os10t0544900-01	0.85	0.13	OsPP114	protein phosphatase 2C72
	Os02t0599700-01	0.82	0.42	OsPP29	protein phosphatase 2C19
	Os07t0507000-01	0.79	0.34	OsPP95	Protein phosphatase 2C.
	Os05t0491200-02	1.43	0.16	akin-b	beta-subunit of SnRK1
	Os02t0178000-01	-3.83	0.05	akin-b	Sucrose nonfermenting-1-related protein kinase 3.9
	Os05t0530500-01	-1.32	0.30	OsSnRK1.2, OSK1	sucrose non-fermenting-1 related protein kinase 1a
	Os12t0586100-01	1.79	0.09	OsSAPK9, OsSnRK2.9	STRESS/ABA-ACTIVATED PROTEIN KINASE 9
	Os03t0250000-02	-1.82	0.10	OsSCS1	SNRK2-CALCIUM SENSOR 1
	Os03t0250000-01	-1.69	0.11	OsSCS1	SNRK2-CALCIUM SENSOR 1
	Os01t0963600-01	-2.77	0.09	OsAsr2	ABA/WDS induced protein family protein
	Os12t0435200-01	-7.71	0.01	OsNCED2	9-CIS-EPOXYCAROTENOID DIOXYGENASE 2
	Os02t0704000-01	-5.32	0.02	OsNCED1	9-CIS-EPOXYCAROTENOID DIOXYGENASE 1
	Os12t0617400-01	-2.48	0.23	OsNCED5	9-CIS-EPOXYCAROTENOID DIOXYGENASE 5
Cold Stress response	Os11t0523700-01	3.34	0.02	OsICE1 bHLH116	Transcription factor ICE1, Basic helix- loop-helix protein 116
	Os02t0231000-00	0.99	0.15	8, AP2/ EREBP82, OsD	ETHYLENE RESPONSE FACTOR 38
	Os04t0549700-01	4.27	0.04	3, AP2/ EREBP40, OsD	Dehydration responsive element binding protein 1F
	Os02t0656600-00	3.52	0.04	OsERF32, AP2/EREBP2	Dehydration responsive element binding protein 2B
	Os01t0165000-02	1.24	0.10	DERB2A	DRE binding protein 2.
	Os02t0752800-02	-1.12	0.02	sERF49, AP2/EREBP13	Dehydration responsive element binding protein 2B
	Os02t0752800-01	-1.05	0.02	sERF49, AP2/EREBP13	Dehydration responsive element binding protein 2B
	Os06t0165600-01	-1.00	0.13	DREB1D	Dehydration responsive element binding protein 1D
	Os06t0165600-01	-1.40	0.22		
Light Signaling, Circ	Os09t0510500-01	4.32	0.01	OsBC1, OsBUL1	BASIC HELIX-LOOP-HELIX PROTEIN 81
	Os04t0350700-01	3.21	0.03	OsbHLH093, AWN1	REGULATOR OF AWN ELONGATION 1
	Os04t0618600-01	1.81	0.18	OsbHLH101, OsPIF1	BASIC HELIX-LOOP-HELIX PROTEIN 101
	Os01t0126600-01	2.89	0.05	OsFDML2	FACTOR OF DNA METHYLATION LIKE 1
	Os06t0275500-01	1.13	0.06	OsCLF	CURLY LEAF
	Os06t0614000-01	2.41	0.09	OsFTIP1	FT-INTERACTING PROTEIN 1
	Os01t0218500-02	3.55	0.19	OsFTL1	FLOWERING LOCUS T (FT)-Like homolog
	Os01t0626400-01	1.68	0.24	OsWRKY11	WRKY transcription factor
	Os03t0445700-01	5.02	0.01	OsLBD37	LATERAL ORGAN BOUNDARIES DOMAIN protein
	Os02t0724000-01	0.91	0.18	OsBBX7	CONSTANS-like protein
	Os04t0304200-01	-4.80	0.00	OsPHOT2	Phototropin
	Os03t0309200-01	-1.17	0.05	OsPHYB	Phytochrome B
	Os03t0752100-01	-1.00	0.08	OsPHYC	Phytochrome C
	Os10t0369600-01	-0.85	0.10	OsGRAS39	GRAS PROTEIN 39
	Os12t0610200-01	-3.17	0.11	OsPIL11	Phytochrome-interacting factor 3
	Os08t0157600-01	-1.01	0.25	OsCCA1	CIRCADIAN CLOCK ASSOCIATED 1
	Os04g0452100	-5.01	0.01	OsCRY1b	Cryptochrome 1b
	Os02t0573200-01	-2.73	0.02	OsCRY1a	Cryptochrome 1
Photosynthesis, Carb	Os07t0141400	-1.26	0.04	OsPsbP	oxygen-evolving enhancer protein 2
	Os01t0501800-1	-1.48	0.00	OsPSBO	oxygen-evolving enhancer protein 1
	Os04t0234600-03	-6.38	0.01	OsSBPase	sedoheptulose-1, 7-bisphosphatase
	Os04t0234600-01	-4.78	0.01	OsSBPase	sedoheptulose-1, 7-bisphosphatase
	Os04t0234600-02	-4.26	0.03	OsSBPase	sedoheptulose-1, 7-bisphosphatase
	Os07t0544800-01	-1.32	0.16	OsPsbQ	oxygen-evolving enhancer protein 3
	Os02g0152400-1	5.50	0.01	OsRBCS1	RuBisCO subunit binding-protein beta subunit
	Os03t0735000-01	-4.11	0.00	OsAGPL1, OsAPL1	ADP-GLUCOSE PYROPHOSPHORYLASE LARGE SUBUNIT 1
	Os07t0243200-01	1.45	0.03	GPL4, OsAPL4, OsSTA	ADP-GLUCOSE PYROPHOSPHORYLASE LARGE SUBUNIT 4
	Os08g0345800-1	-2.44	0.03	OsAGPS2a	ADP-GLUCOSE PYROPHOSPHORYLASE LARGE SUBUNIT 2
	Os08g0345800-4	-1.52	0.10	OsAGPS2a	ADP-GLUCOSE PYROPHOSPHORYLASE LARGE SUBUNIT 3
	Os06t0160700-01	-1.29	0.22	OsSSI	SOLUBLE STARCH SYNTHASE I
	Os06t0229800-01	4.18	0.03	OsSSIIa	SOLUBLE STARCH SYNTHASE IIa
	Os08g0191433-00	2.03	0.06	OsSSIIIa	SOLUBLE STARCH SYNTHASE IIIa
	Os06g0133000-01	-0.89	0.22	OsGBSS1	Granule-bound starch synthase
	Os05g0438600	-1.20	0.22	OscFBP2	CYTOSOLIC FRUCTOSE-1,6-BIPHOSPHATE 2
	Os01g0905800	0.82	0.16	ALDC1	CYTOPLAST ALDOLASE 1
	Os11g0171300-02	-2.40	0.07	OsFBAase, OsALDO	CHLOROPLAST ALDOLASE
	Os11g0171300-01	-1.88	0.09	OsFBAase, OsALDO	CHLOROPLAST ALDOLASE
ROS Detoxification	Os11t0112400-01	5.15	0.01	OsPRX2	class III peroxidase 130
	Os03t0434800-00	6.54	0.02	OsPRX2	Peroxidase 2
	Os01t0326000-02	3.85	0.09	OsPRX12	class III peroxidase 12
	Os02t0236600-01	5.05	0.02	OsPRX27	class III peroxidase 27
	Os05t0134400-02	3.39	0.06	OsPrx65	class III peroxidase 65
	Os05t0162000-01	1.71	0.01	OsPrx72	PEROXIDASE 72
	Os06t0547400-01	2.04	0.09	OsPRX86	class III peroxidase 86
	Os10t0109300-01	5.32	0.00	OsPRX125	class III peroxidase 125
	Os10t0109600-01	0.69	0.17	OsPrx126	class III peroxidase 126
	Os10t0536700-01	4.05	0.03	OsPRX128	class III peroxidase 128
	Os11t0210100-01	3.46	0.09	OsPRX133	class III peroxidase 133
	Os03t0285700-01	1.12	0.19	OSAPX1	L-ascorbate peroxidase 1
	Os02t0115700-01	-1.64	0.08	OsCatA	Catalase isozyme A
Ion, Water Transport	Os01t0249200-01	5.77	0.01	OsGLP1-1	GERMIN-LIKE PROTEIN 1-1
	Os07t0522600-02	0.90	0.01	OsGLR3.7	Glutamate receptor 3.4
	Os02t0117500-01	1.40	0.04	OsGLR3.1, OsGLR3.2	GLUTAMATE RECEPTOR-LIKE 3.2
	Os07t0103100-01	-2.26	0.02	OsGLR3.6, OsGLR3.4	GLUTAMATE RECEPTOR-LIKE 3.4
	Os04t0585200-01	-2.46	0.04	OsGLR3.2, OsGLR3.1	GLUTAMATE RECEPTOR-LIKE 3.1
	Os06t0188800-01	-2.29	0.04	OsGLR4.4	Glutamate receptor homolog 4.4
	Os06t0680500-01	-2.02	0.04	OsGLR3.5, OsGLR3.3	GLUTAMATE RECEPTOR-LIKE 3.3
	Os02t0787600-01	-2.37	0.05	OsGLR1.2, OsGLR1.4	GLUTAMATE RECEPTOR-LIKE 1.4
	Os04t0233400-01	4.49	0.04	OsPIP2	PLASMA MEMBRANE INTRINSIC PROTEIN 2;6
	Os06t0716800-01	-1.48	0.00	OsbZIP53	b-ZIP TRANSCRIPTION FACTOR 53
	Os09t0541000-01	-4.66	0.02	OsPIP2-6	PLASMA MEMBRANE INTRINSIC PROTEIN 2;7
	Os09t0541000-02	-3.50	0.02	OsPIP2-6	PLASMA MEMBRANE INTRINSIC PROTEIN 2;8
	Os02t0823100-01	-2.18	0.19	OsPIP1-3	PLASMA MEMBRANE INTRINSIC PROTEIN 1;3
Stomata size	Os0t0485500-01	3.68	0.01	OsEPFL1, EPFL1, GAD	Epidermal patterning factor-like 1
	Os01t0914400-01	1.95	0.33	MAGEN, OsEPFL9, EP	Epidermal Patterning Factor like-9

968   **Table S1. Expression level of Transcripts of some selected pathway from microarray analysis in rice.** Flag
969   leaves on the day of final emergence of the panicle from the CNP treated and untreated plant were sampled with
970   liquid N2 after 4th CNP treatment. Microarray analysis was done from two biological replicates each category.
971   Normalization and Fold change was calculated as described in the materials and methods section. Transcript
972   details are taken from Rice Annotation Project Database (RAP-DB). Pathway analysis was done using GO
973   Ontology, KEGG and Biological Analysis tool DAVID (http://david.abcc.ncifcrf.gov/)

Table S2. Expression level of Transcripts of some selected pathway from transcriptome sequencing analysis in Arabidopsis thaliana. 16-day old CNP seedlings from two biological replicates each category of treated and untreated were sampled with liquid N2 for transcriptome sequencing. Normalization and Fold change was calculated as described in the materials and methods section. Transcript details are taken from TAIR database.

Pathway / Process Inve	ID (Arabido	Log₂ FC	P-value	Gene Symbol	Gene Name
ABA pathway	AT4G34000	1.20	0.004	ATABF3	ABSCISIC ACID RESPONSIVE ELEMENTS-BINDING FACTOR 3
	AT1G07430	2.38	0.000	ATAIP1	AKT1 INTERACTING PROTEIN PHOSPHATASE 1
	AT3G21780	-1.48	0.018		UDP-glycosyltransferase 71B6
	AT1G68765	-5.42	0.000	IDA	INFLORESCENCE DEFICIENT IN ABSCISSION
	AT4G27920	-1.10	0.629	PYL10, RCAR4	PYR1-LIKE 10
	AT1G70810	-1.27	0.008	CAR7	Protein C2-DOMAIN ABA-RELATED 7
	AT3G44860	-3.06	0.000	FAMT	FARNESOIC ACID CARBOXYL-O-METHYLTRANSFERASE
	AT5G53820	-2.48	0.009	LEA	Late embryogenesis abundant protein
	AT1G48590	-1.53	0.771	CAR5	C2-DOMAIN ABA-RELATED 5
	AT3G14440	1.44	0.001	ATNCED3	NINE-CIS-EPOXYCAROTENOID DIOXYGENASE 3
	AT4G19170	1.19	0.009	CCD4, NCED4	NINE-CIS-EPOXYCAROTENOID DIOXYGENASE 4, CAROTENOID CLEAVAGE DIOXYGENASE 4
	AT4G18350	-1.17	0.512	ATNCED2	NINE-CIS-EPOXYCAROTENOID DIOXYGENASE 2
Cold Stress Response	AT2G38340	-2.84	0.219	DREB2E, DREB19, ERF046	Dehydration-responsive element-binding protein 2E, Dehydration response element-binding protein 19
	AT1G63030	-1.85	0.029	DREB1E, DDF1, ERF032	Dehydration-responsive element-binding protein 1E
	AT1G43160	-1.84	0.155	RAP2-6, ERF108	Ethylene-responsive transcription factor RAP2-6
	AT5G04340	-1.49	0.000	ZAT6, CZF2	Zinc finger protein ZAT6 (COLD INDUCED ZINC FINGER PROTEIN 2)
	AT5G58670	-1.43	0.029	PLC1	Phosphoinositide phospholipase C 1
	AT1G77120	-1.27	0.003	ADH1	Alcohol dehydrogenase class-P
	AT3G50260	-1.09	0.044	ERF011	Ethylene-responsive transcription factor ERF011
	AT3G50980	3.65	0.082		Dehydrin Xero 1
Light Signaling, Circa	AT5G52390	-3.33	0.002	PAR1	Photoassimilate-responsive protein PAR-like protein
	AT1G18810	1.54	0.027	PKS3	PHYTOCHROME KINASE SUBSTRATE 3
	AT2G43010	2.55	0.000	PIF4	Phytochrome interacting factor 4
	AT5G04190	2.77	0.001	PKS4	PHYTOCHROME KINASE SUBSTRATE 4
	AT1G24590	1.75	0.354	ESR2	Ethylene-responsive transcription factor
	AT3G22231	-2.72	1.53068E-08	PCC1	PATHOGEN AND CIRCADIAN CONTROLLED 1
Photosynthesis, Chlor	AT1G29930	1.31	0.147	LHCB1.3, CAB1	Chlorophyll a-b binding protein 1
	AT3G47470	1.59	0.002	LHCA4, CAB4	Chlorophyll a-b binding protein 4
	AT1G29920	3.14	0.000	LHCB1.2, CAB3	Chlorophyll a-b binding protein 3
	AT5G23950	2.11	0.293	MRO11.1	Calcium-dependent lipid-binding family protein
	AT2G34430	2.45	0.000	LHB1B1	LIGHT-HARVESTING CHLOROPHYLL-PROTEIN COMPLEX II SUBUNIT B1
	AT5G54190	2.06	0.003	PORA	NADPH-protochlorophyllide oxidoreductase
	AT3G54890	1.05	0.023	LHCA1	PHOTOSYSTEM I LIGHT HARVESTING COMPLEX GENE 1
	AT1G15820	1.30	0.011	CP24, LHCB6	LIGHT HARVESTING COMPLEX PHOTOSYSTEM II SUBUNIT 6
	AT3G08940	1.24	0.010	LHCB4.2	LIGHT HARVESTING COMPLEX PHOTOSYSTEM II
	AT1G61520	1.30	0.007	LHCA3	PHOTOSYSTEM I LIGHT HARVESTING COMPLEX GENE 3
	AT5G54270	1.68	0.000	LHCB3	LIGHT-HARVESTING CHLOROPHYLL B-BINDING PROTEIN 3
	AT1G03130	1.20	0.006	PSAD-2	PHOTOSYSTEM I SUBUNIT D-2
	AT2G34420	2.24	0.000	LHB1B2	PHOTOSYSTEM II LIGHT HARVESTING COMPLEX GENE B1B2
	AT1G29910	1.91	0.000	CAB3, LHCB1.2	CHLOROPHYLL A/B BINDING PROTEIN 3, LHCB1.2
	AT2G05070	1.97	0.000	LHCB2	LIGHT-HARVESTING CHLOROPHYLL B-BINDING 2
	AT2G05100	2.02	0.000	Lhcb2.1, LHCB2.3	allele of LHCB2.1
	AT3G27690	1.53	0.000	LHCB2.3, LHCB2.4	PHOTOSYSTEM II LIGHT HARVESTING COMPLEX GENE 2.3
	AT5G24410	2.41	0.366	PGL4	6-phosphogluconolactonase
	AT1G44446	1.21	0.003	CAO	Chlorophyllide a oxygenase
	AT2G18700	1.03	0.018	TPS11	TREHALOSE PHOSPHATASE/SYNTHASE 11
	AT1G71380	2.06	0.082	CEL3	Endoglucanase 9, Cellulase 3
	AT3G21370	2.73	0.129	BGLU19	BETA GLUCOSIDASE 19
	AT4G27550	1.10	0.950	TPS4	Trehalose-6-phosphate synthase 4
	AT1G61800	-2.35	0.000	ATGPT2	Glucose-6-phosphate/phosphate translocator 2
	AT2G02810	-2.04	0.000	UTR1	UDP-galactose/UDP-glucose transporter 1
	AT4G39210	-1.05	0.017	APL3	large subunit of ADP-Glucose Pyrophosphorylase
	AT1G12600	-1.11	0.360	UTR4	UDP-galactose/UDP-glucose transporter 4
	AT1G05530	-1.93	0.375	UGT75B2, UGT2	UDP-glycosyltransferase 75B2, Indole-3-acetate beta-glucosyltransferase 2
	AT5G11670	-1.54	0.000	AtNADP-ME2	NADP-MALIC ENZYME 2
	AT1G53310	-1.38	0.001	ATPEPC1	Phosphoenolpyruvate carboxylase
	AT2G40100	-1.65	0.000	LHCB4.3	LIGHT HARVESTING COMPLEX PHOTOSYSTEM II
	AT5G19550	-1.33	0.001	AAT2, ASP2	ASPARTATE AMINOTRANSFERASE 2
	AT4G18360	-1.44	0.014	GOX3	GLYCOLATE OXIDASE 3
	AT5G63680	-1.04	0.013		Pyruvate kinase
	AT4G26270	-1.26	0.006	PFK3	Phosphofructokinase
	AT1G05610	-1.37	0.219	APS2	small subunit of ADP-glucose pyrophosphorylase.
ROS Detoxification	AT2G28190	0.99	0.040	ATSOD2	SUPEROXIDE DISMUTASE 2
	AT4G35090	1.16	0.009	CAT2	CATALASE 2
	AT3G49120	-3.23	0.000	ATPERX34	PEROXIDASE 34
	AT5G64120	-2.30	0.000	ATPRX71	PEROXIDASE 71
	AT5G05340	-6.74	0.000	PRX52	PEROXIDASE 52
	AT4G08770	-4.20	0.000	PRX37	Peroxidase 37
Ion, Water Solute Tra	AT2G25810	-1.40	0.064	TIP4-1	Aquaporin
	AT5G47450	1.11	0.365	TIP2-3	Aquaporin
	AT4G13510	-1.31	0.002	AMT1-1	Ammonium transporter 1
	AT3G47420	-1.95	0.000	AtPS3	PHOSPHATE STARVATION-INDUCED GENE 3
	AT1G61800	-2.35	0.000	ATGPT2	GLUCOSE6-PHOSPHATE PHOSPHATE TRANSLOCATOR 2
	AT2G02810	-2.04	0.000	UTR1	UDP-galactose/UDP-glucose transporter 1
	AT1G35350	-1.38	0.002	PHO1-H8	Phosphate transporter PHO1 homolog 8
	AT1G26730	-1.45	0.003	PHO1-H7	Phosphate transporter PHO1 homolog 7
	AT5G51050	-1.12	0.012	APC2	Calcium-dependent mitochondrial ATP-magnesium/phosphate carrier protein 2
	AT2G32830	-2.65	0.001	PHT5	PHOSPHATE TRANSPORTER 1;5
	AT3G48850	-2.66	0.001	PHT3	PHOSPHATE TRANSPORTER
	AT5G43370	-1.65	0.182	PHT1;2	PHOSPHATE TRANSPORTER 2
	AT1G20860	-4.75	0.006	PHT1;8	Phosphate transporter 18
	AT2G29650	1.28	0.014	ANTR1 PHT4;1	Sodium/phosphate cotransporter 1
	AT1G76430	-4.68	0.005	PHT1-9	H(+)/Pi cotransporter
	AT3G56200	-1.30	0.003	AVT6C	Amino acid transporter
	AT4G02050	-1.03	0.021	STP7	Hexose transporter 7
	AT1G55910	-1.14	0.028	ZIP11	Zinc transporter 11
	AT3G63380	-2.68	0.000	ACA12	AUTO-INHIBITED CA2+ ATPASE 12
	AT3G22910	-1.07	0.094	ACA13	calcium-transporting ATPase 13
	AT3G23870	-1.27	0.107	ENOR3L2	magnesium transporter
	AT3G45700	-2.53	0.348	NPF2.4	nitrate excretion transporter 5
	AT1G70335	-2.40	0.348	ENT1	Equilibrative nucleotide transporter 1
	AT3G45650	-1.88	0.000	NAXT1	Nitrate excretion transporter1
	AT3G21670	1.50	0.002	NRT1.3, AtNPF6.4	Nitrate transporter
	AT3G21260	1.02	0.031	GLTP3	Glycolipid transfer protein 3
	AT2G25680	1.26	0.091	MOT1	Molybdate transporter 1
	AT4G25010	-2.16	0.130	SWEET14	Bidirectional sugar transporter
	AT5G13170	2.36	0.033	SWEET15, SAG29	Bidirectional sugar transporter, Senescence-associated protein
	AT5G03570	-1.33	0.445	IREG2, FPN2	FERROPORTIN 2
	AT2G01770	2.14	0.102	VIT1	VACUOLAR IRON TRANSPORTER 1
	AT4G19690	1.67	0.286	IRT1	Iron-regulated transporter 1
	AT4G18790	1.15	0.951	NRAMP5	Metal transporter
	AT4G32510	2.45	0.073	BOR7	boron transporter 7
	AT1G78000	-1.44	0.008	SULTR1;2	SULFATE TRANSPORTER
	AT1G22150	-2.22	0.003	SULTR1;3	SULFATE TANSPORTER SULTR1;3
	AT1G77992	1.16	0.733	SULTR2;2	Sulfate transporter 2.2
Stomata size	AT3G13898	1.90	0.364	EPFL3	EPIDERMAL PATTERNING FACTOR-like protein 3

974

975 **Table S2. Expression level of Transcripts of some selected pathway from transcriptome sequencing analysis**
976 **in Arabidopsis thaliana.** 16-day old CNP seedlings from two biological replicates each category of treated and
977 untreated were sampled with liquid N2 for transcriptome sequencing. Normalization and Fold change was
978 calculated as described in the materials and methods section. Transcript details are taken from TAIR database.

979 **Table S3. Primers used in this study**

980

981

982